Earth-Science Reviews 235 (2022) 104251

Contents lists available at ScienceDirect

Earth-Science Reviews

journal homepage: www.elsevier.com/locate/earscirev

Latest Cretaceous palaeogeographic evolution of northeast Iberia: Insights from the Campanian continental Montalbán subbasin (Spain)

Marcos Aurell[a,*], Diego Torromé[a], José M. Gasca[b], Pablo Calvín[c], Manuel Pérez-Pueyo[a], Jara Parrilla-Bel[a], Eduardo Medrano-Aguado[a], Carles Martín-Closas[d], Alba Vicente[e], Pablo Sierra-Campos[c], José I. Canudo[a]

[a] Departamento de Ciencias de la Tierra-IUCA (Grupo Aragosaurus), Universidad de Zaragoza, 50009 Zaragoza, Spain
[b] Departamento de Geología, Universidad de Salamanca, 37008 Salamanca, Spain
[c] Instituto Geológico y Minero de España-CSIC, Unidad de Zaragoza, C/Manuel Lasala 44, 50006 Zaragoza, Spain
[d] Departament de Dinàmica de la Terra i de l'Oceà, Facultat de Ciències de la Terra, 08028 Barcelona, Spain
[e] Instituto Politécnico Nacional, 23096 La Paz, Baja California Sur, Mexico

ARTICLE INFO

Keywords:
Latest Cretaceous
Iberia
Tecto-sedimentary evolution
Dinosaurs
Magnetostratigraphy

ABSTRACT

This work characterizes for the first time the 500–700 m-thick uppermost Cretaceous continental sedimentary succession of the Allueva Fm recorded in the northeastern margin of the Iberian basin, in the Montalbán subbasin (Maestrazgo domain, Spain). The middle-upper Campanian age of this unit constrained here by new paleomagnetic and biostratigraphic data involves major revision of previous stratigraphic and palaeogeographic interpretations. The uplift of the northern marginal areas of the Montalbán subbasin onwards from the middle Campanian supplied the coarse terrigenous-clastic sediments common in the alluvial Allueva Fm. Moreover, a sharp increase of the sedimentation rates (from 4 to 19 cm/ky) from the lower to the middle-upper part of the Allueva Fm has been related to further increase of the tectonic activity during the middle part of the late Campanian. Also relevant are the new discovered vertebrate sites mostly found in the marginal areas of a large lacustrine-palustrine carbonate system developed during the latest Campanian. Vertebrate sites include a fossil assemblage with abundance of titanosaur sauropod dinosaurs as well as the presence of ornithopod dinosaurs and crocodylomorphs. A review of the dinosaur fossil sites recorded in other Iberian subbasins shows a similar fossil assembage occurrence during the late Campanian–earliest Maastrichtian timespan, previous to the faunal turnover that took place in the Ibero-Armorican landmass around the onset of the late Maastrichtian. The stratigraphic, sedimentological and paleontological characterization of the successions recorded during the initial stages of development of the Montalbán subbasin have major implication to understand the latest Cretaceous palaeogeographic evolution of northeast Iberia. Comparative review to other latest Cretaceous continental successions deposited in other domains of the Iberian basin indicates a south to north migration of newly developed subsident subbasins: during the Campanian (South Iberian domain), during the middle-late Campanian (northern Maestrazgo domain), and during the Maastrichtian (central Castillian domain).

1. Introduction

The latest Cretaceous onset of Africa-Europe-Iberia convergence caused the structuration of the first thrust sheets in the Pyrenees, with the initial development of the associated foreland basins at the end of the Santonian (e.g. Dercourt et al., 1986; Visser and Meijer, 2012; Dielforder et al., 2019; Martín-Chivelet et al., 2019a). After this initial compressive stage, the decrease of the tectonic activity during the Paleocene involved relatively low subsidence rates (Garcés et al., 2020), and favoured the setting of extensive progradational shallow carbonate platforms in the southern margin of the Basque-Cantabrian domain (Baceta et al., 1999, 2005). This stage of relative tectonic quiescence (or stasis phase in Dielforder et al., 2019; Fig. 1A) was followed by intense continental margin collision during the Eocene, with sharp increase of subsidence and sedimentation rates in the South Pyrenean foreland basin (e.g. Puigdefàbregas et al., 1986; Garcés et al., 2020 and references

* Corresponding author.
E-mail address: maurell@unizar.es (M. Aurell).

https://doi.org/10.1016/j.earscirev.2022.104251
Received 4 July 2022; Received in revised form 4 November 2022; Accepted 7 November 2022
Available online 15 November 2022

therein). This plate convergence had also impact in the interior areas of northeast Iberia, with the progressive inversion and contractive deformation of the Mesozoic Iberian basin rift system giving rise to the alpine Iberian Ranges (e.g. Alvaro et al., 1979; Vegas et al., 2019).

Continental to coastal sedimentary settings covered wide areas of northeast Iberia during latest Cretaceous. The alluvial to lacustrine-palustrine successions recorded in these areas have variable thickness and different age ranges within the Campanian–Maastrichtian timespan. These successions include local terrestrial vertebrate sites with dinosaur fossils, which have been studied over the last decades (Fig. 1B). Numerous sites have been described in the South-central Pyrenean domain (e.g. Llompart et al., 1984; López-Martínez et al., 2001; Fondevilla et al., 2019; Pérez-Pueyo et al., 2021), and south to the Basque-Cantabrian basin, between the Villarcallo-Treviño localities (e.g. Bardet et al., 1997; Astibia et al., 1999; Berreteaga, 2008; Berreteaga et al., 2011; Pereda-Suberbiola et al., 2015). Continental-dominated successions are also found in separated domains of the Iberian basin. Northwards, in the *Castillian domain*, the Santibañez del Val Fm includes fossil sites around Santo Domingo de Silos and Talveila areas (e.g. Lapparent et al., 1957; Pereda-Suberbiola and Ruiz-Omeñaca, 2001). To the west, the Vegas de Matute Fm of the *Duero domain* includes the Armuña fossil site (Buscalioni and Martínez-Salanova, 1990; Pérez-García et al., 2016). Southwards, in the *South Iberian domain* are found the fossil sites of Sacedón and Lo Hueco in the Villalba de la Sierra Fm (e.g. Ortega and Pérez-García, 2009; Ortega et al., 2015), as well as different continental vertebrate sites in the Sierra Perenchiza Fm around the localities of Buñol and Chera (e.g. Company, 2004; Company and Szentesi, 2012; Company, 2017). In the southern Iberian margin (in the Prebetic domain), dinosaur fossil tracks have been described near Yecla (Herrero et al., 2016). In the western Iberian margin (northern Lusitanian basin), Campanian–Maastrichtian dinosaur remains are found around the localities of Taveiro, Viso and Aveiro (Antunes and Pais, 1978; Antunes and Mateus, 2003).

The Aliaga and Montalbán subbasins are two highly subsident intramountain troughs located in the northeastern Iberian Ranges, in the northern part of the *Maestrazgo domain* (Fig. 1B). Around the end of the last century, stratigraphic analysis and regional correlation of the thick continental successions recorded in these two subbasins concluded that they were deposited onwards from the late Paleocene (e.g. Pardo et al., 1989, 2004; Casas et al., 2000; Muñoz et al., 2002). Later on, Canudo et al. (2005) reported the finding of a paleontological site with dinosaurs and testudines near the locality of Cirugeda, in the northern part of the Aliaga subbasin. This isolated discovery was of high relevance, because it challenged the late Paleocene–middle Eocene age given for this site in previous works (e.g. Pardo et al., 1989). Here we report on further discovery of new vertebrate fossil sites (including abundant dinosaurs) located in the northern part of the Montalbán subbasin. The stratigraphic interval including these new dinosaur sites was previously assigned to the middle Eocene (Pardo et al., 1989; Casas et al., 2000; Gónzalez and Pérez, 2018). Therefore, since all non-avian dinosaur got extinct after the K/Pg event, at the end of the Maastrichtian (e.g. Brusatte et al., 2015), the dinosaur discoveries reported here involve a major stratigraphic review and updating of the continental units deposited during the initial stages of development of the Montalbán subbasin.

This work characterizes the sedimentary succession with dinosaur sites found in the northern part of the continental Montalbán subbasin. This succession is now placed in a precise stratigraphic, sedimentological, and palaeogeographic framework. The data reported here were acquired after a multidisciplinary approach, with lithostratigraphic logging and correlation supported by detailed geological mapping in well exposed and continuous outcrops combined to age calibration

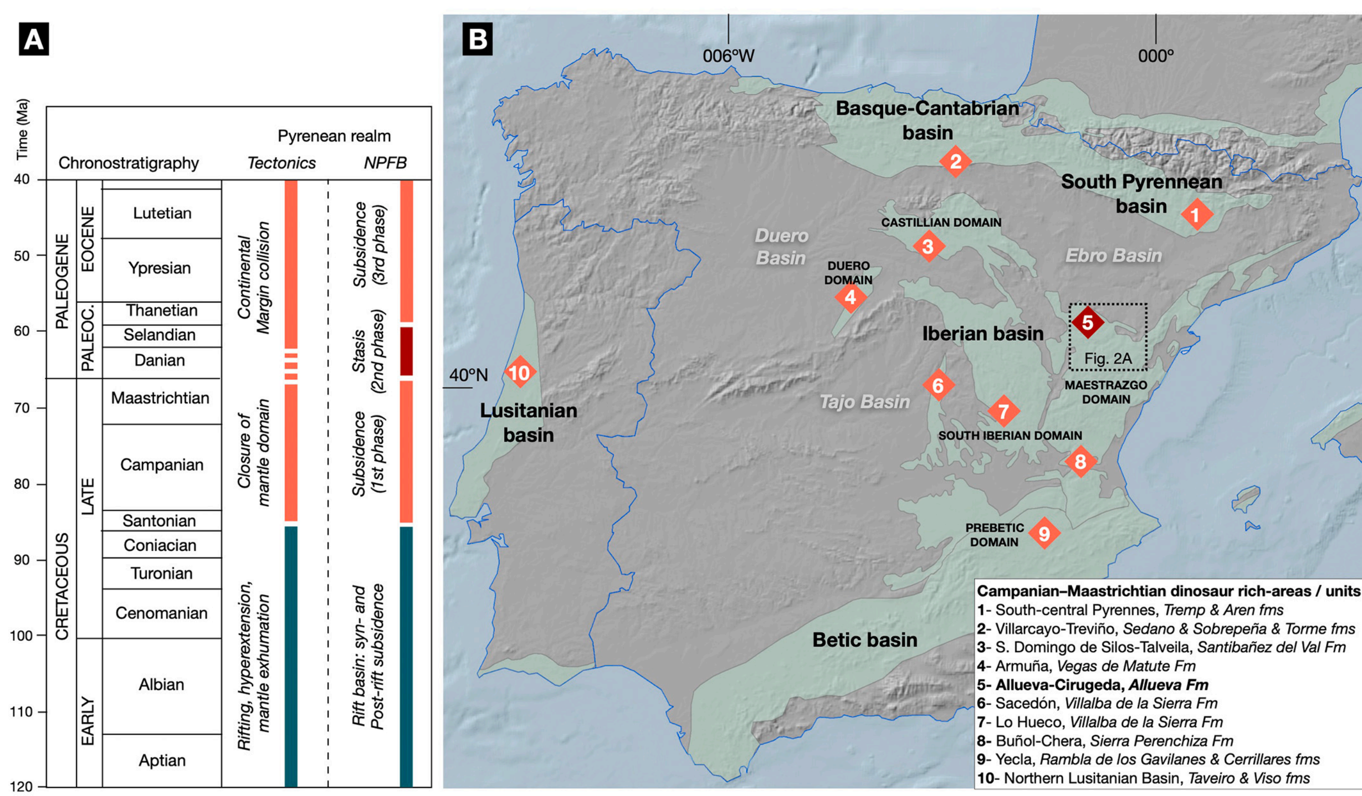

Fig. 1. **A.** Tectonic evolution in the Pyrenean realm and subsidence phases in the north Pyrenean foreland basin (NPFB) during the Cretaceous-Paleogene (modified from Dielforder et al., 2019). **B:** Distribution of the Mesozoic sedimentary basins of Iberia. Green areas show the overall distribution of the Mesozoic-Paleogene outcrops (modified from Aurell et al., 2019). Numbers indicate the location of areas with fossil sites including Campanian-Maastrichtian dinosaurs. (For interpretation of the references to colour in this figure legend, the reader is referred to the web version of this article.)

based in new palaeomagnetic and biostratigraphic data. The obtained data lead to the definition of the middle-upper Campanian terrigenous-dominated alluvial Allueva Fm. The accurate stratigraphic characterization reached here for the Allueva Fm allows the correlation and comparison with other uppermost Cretaceous dinosaur-bearing units found in the different sedimentary domains of the Iberian basin. In particular, the characterization of the sedimentary succession recorded during the initial stage of development of the Montalbán subbasin combined to the comparative review presented here have major impact to document the palaeogeographic evolution of northeastern Iberia at the end of the Cretaceous. In this work, different aspects are addressed concerning the stratigraphy, paleontology and palaeogeographic evolution of northeast Iberia during the latest Cretaceous.

2. Geological setting

Tectonic extension during most of the Mesozoic in northeast Iberia resulted in the development of the Iberian basin rift system (e.g. Alvaro et al., 1979; Liesa et al. in Martín-Chivelet et al., 2019b; Aurell et al., 2019). The Mesozoic evolution of this basin is regarded as having three episodes of continental rifting during the Triassic, the Kimmeridgian–Berriasian, and the Barremian–early Aptian (Salas et al. in Martín-Chivelet et al., 2019b). Wide shallow marine carbonate platforms developed during intermediate stages of post-rift thermal-dominated subsidence, shuch as the Jurassic or Late Cretaceous.

The Iberian basin rift system was inverted during the alpine compression, giving rise to the Iberian Ranges. These ranges are bounded to the north by the Ebro basin, which corresponds to the main foreland basin of the Pyrenean orogeny, and to the west by two large intraplate Cenozoic depressions of the Tajo and Duero basins (Fig. 1B). The initial latest Cretaceous stages of inversion of the Iberian basin are broadly described in synthesis works (García et al., 2004; Martín-Chivelet et al., 2019a). Moreover, several works emphasize on the role of the main phase of the alpine compressional deformation during the Eocene–early Miocene building-up the Iberian Ranges, with precise documentation of the coeval development and sedimentary filling of separated intramountain continental basins and subbasins (e.g. González and Guimer, 1993; Casas et al., 2000; Capote et al., 2002; Guimerà et al., 2004; Antolín-Tomás et al., 2007; Guimerà, 2018; Liesa et al., 2018).

The Montalbán anticline is an alpine compressive structure located in the northeastern part of the Iberian Ranges (Fig. 2A). This large asymmetrical anticline structure involves Palaeozoic rocks previously folded and thrusted during the Variscan orogeny, and is in continuity (to the northwest) with a NW-SE Palaeozoic-cored structure that has an outcropping length of about 150 km and a width of between 5 and 30 km (Casas et al., 2000). A number of compressional intramountain troughs or subbasins of variable size are found around the Montalbán anticline. The Montalbán and Aliaga subbasins developed southwest to this anticline, whereas northwards are found the Muniesa, Alloza, and Berge subbasins. Further north, the Sierra de Arcos thrust system marks the boundary with the southeastern sector of the Cenozoic foreland Ebro

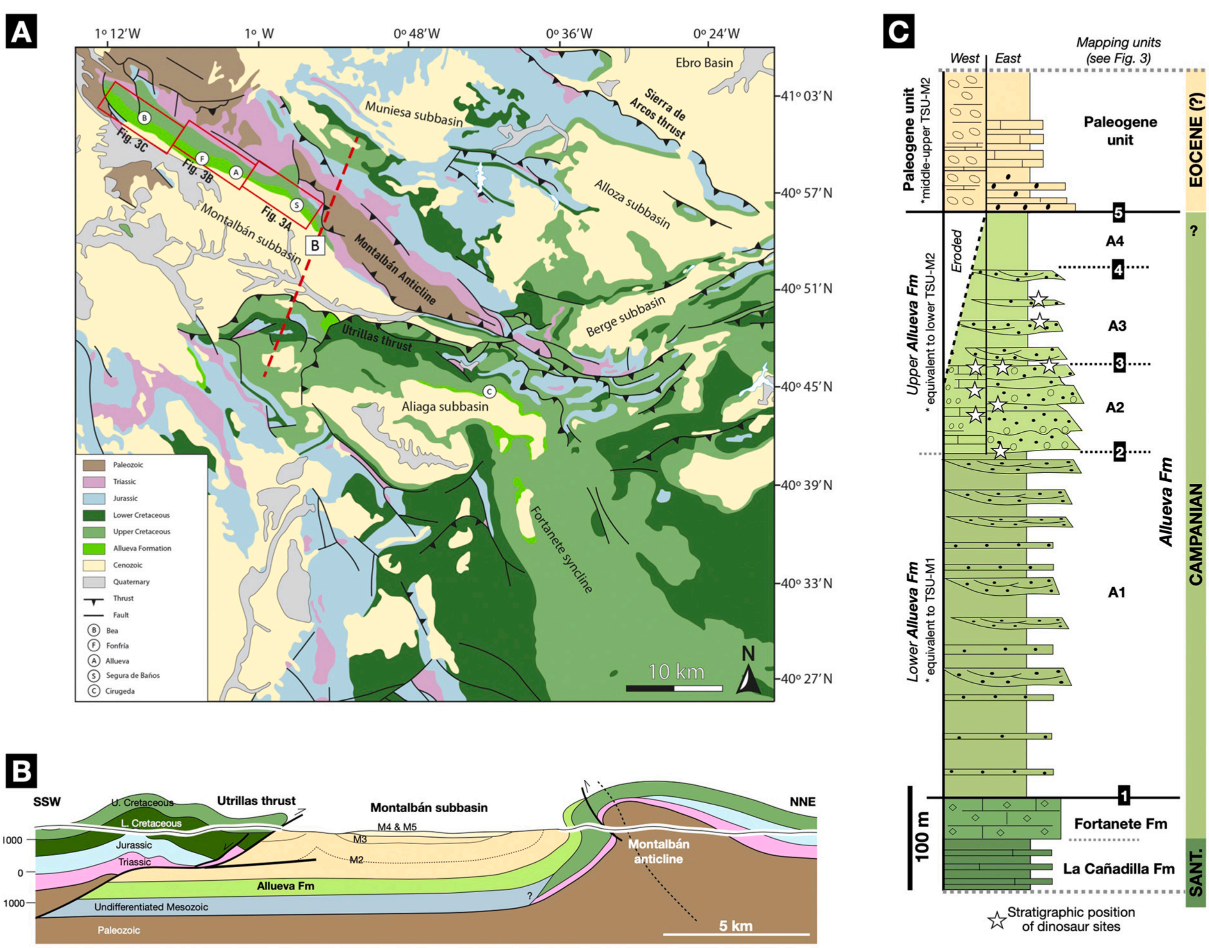

Fig. 2. A: Geological map around the study area (in red rectangles, see Fig. 1 for location), indicating the distribution of the outcrops of the Allueva Fm in the Montalbán and Aliaga subbasins, and in the core of the Fortanete syncline (modified after Torromé et al., 2022). **B:** Cross-section across the central Montalbán subbasin (see A for location; modified from Casas et al., 2000). **C:** Synthetic log updating the uppermost Cretaceous stratigraphy of the study area (ages partly based in data reported in this work). (For interpretation of the references to colour in this figure legend, the reader is referred to the web version of this article.)

basin (Casas et al., 1997; Aurell et al., 2018). The Montalbán subbasin studied here is c. 50 km in length. It is bounded to the north by the Montalbán anticline, and to the south by the Utrillas thrust (Fig. 2B). Towards the east the subbasin narrows at the intersection between these two structures. The Montalbán subbasin forms an overall syncline structure whose northern, steeply-dipping limb coincides with the southern limb of the Montalbán anticline. The southern horizontal limb of the syncline is overthrusted by the Utrillas thrust (Casas et al., 2000).

The uppermost Cretaceous of the area located south to the Montalbán anticline consists of three lithostratigraphic units (Fig. 2C). The La Cañadilla Fm (c.60 m-thick) was regarded as deposited during the late Santonian–earliest Campanian (Almunia et al., 1985; García et al., 2004), or during the Santonian (Floquet, 1991; Martín-Chivelet et al., 2019a). Recently, Torromé et al. (2022) indicated a middle Santonian–earliest Campanian age for La Cañadilla Fm based in strontium isotopic data obtained from well-preserved rudist shells, combined to biostratigraphic data collected around the study area. According to Torromé et al. (2022), the Santonian–Campanian boundary is located near the top of the formation. The La Cañadilla Fm is overlain by the Fortanete Fm, a palustrine-lacustrine unit dominated in the study area by poorly bedded intraclastic limestones with abundant black pebbles and terrestrial gastropods. The Fortanete Fm was considered to be mostly Campanian in age (e.g. García et al., 2004; Martín-Chivelet et al., 2019a).

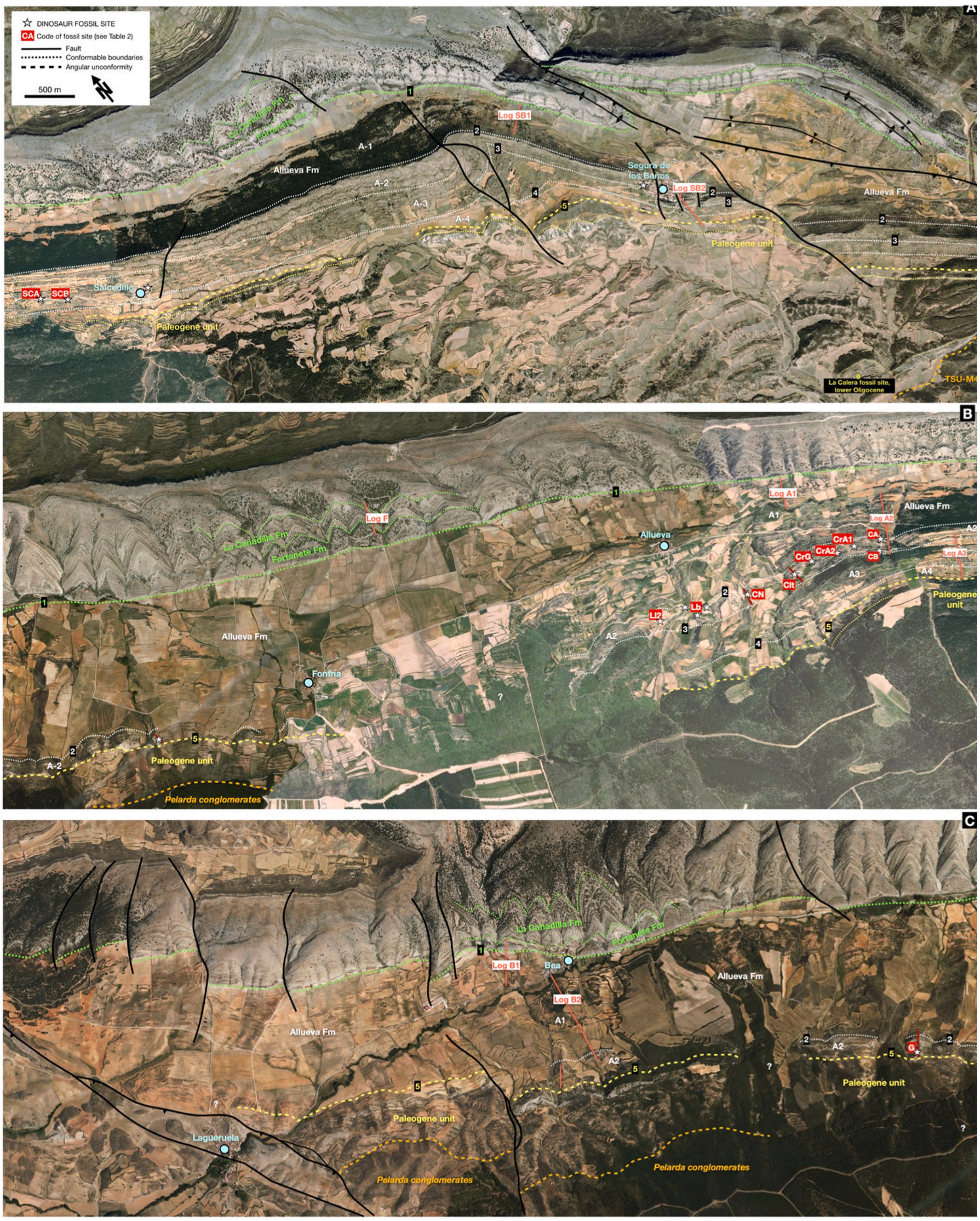

Fig. 3. Distribution of the uppermost Cretaceous–Paleogene units in the aerial images of the area studied between the villages of Segura de los Baños-Salcedillo (**A**), Allueva-Fonfría (**B**) and Bea-Lagueruela (**C**). See Fig. 1 for location. The number of the boundaries of lithostatigraphic units correspond to those in Fig. 2C. White numbers in red squares indicates the codes of dinosaur sites (see Table 2). The location of the logged sections is also indicated. (For interpretation of the references to colour in this figure legend, the reader is referred to the web version of this article.)

The terrigenous-dominated continental sedimentary record of the Montalbán subbasin found above the Fortanete Fm consists of a c.2 km-thick succession of alluvial deposits, varying from conglomerates and sandstones at the basin margins to sandstones and mudstones in intermediate positions, and to lacustrine limestones and gypsum at the basin centre. Pérez et al. (1983) divided this continental succession in five genetic or tecto-sedimentary units (TSUs) M1–M5 bounded by surfaces that mark changes in the vertical sedimentary trend (i.e. from coarsening to finning upward evolutions). The studied uppermost Cretaceous Allueva Fm found in the lower part of this succession is equivalent to the TSU-M1 and to the lower part of the TSU-M2 of Pérez et al. (1983). The Allueva Fm conformably overlain the palustrine carbonates of the Fortanete Fm, whereas its upper boundary is a low-angle erosive unconformity. Above this unconformity rest a c.1 km-thick conformable succession of Paleogene conglomerates, sandstones, mudstones, and limestones with abundant vertical root traces assigned in previous work to the middle and upper part of the TSU-M2 (Pérez et al., 1983). Casas et al. (2000) regarded this unit as deposited during the middle-late Eocene. The palustrine-lacustrine carbonate levels found in the uppermost part of TSU-M2 includes a lower Oligocene charophyte assemblage south of Segura de los Baños (Adrover et al., 1982; La Calera fossil site, see Fig. 3A for location).

3. Material and methods

The reconstruction of the latest Cretaceous sedimentary evolution of the Montalbán subbasin is based on stratigraphical, sedimentological, and palaeontological and palaeomagnetic data collected after extensive field work, geological mapping, and logging in the newly defined Allueva Fm. The key features of this formation are summarized in Table 1. The Allueva Fm has been studied in a continuous 28 km-long NE-SW trending outcrop that exposes the northern margin of Montalbán subbasin, between the villages of Segura de los Baños and Bea (Fig. 2A).

To perform our research we have applied a number of methodological approaches, including: (1) geological mapping of the study area combining fieldwork and analysis of high-resolution aerial imagery; (2) lithostratigraphical and facies analysis after correlation of three successions of the Allueva Fm logged near the villages of Segura de los Baños, Allueva, and Bea, complemented with detailed logging of fossil-rich intervals found in the upper part of the Allueva Fm; (3) palaeontological fieldwork, with the recovery of macro-vertebrate remains by surface collection, and location within the geological framework of the new described dinosaur fossil sites (no site fossiliferous has been excavated, at the moment); (4) microfossil sampling of fine-grained lithologies lithologies in selected horizons (screen-washed samples of 2–5 kg in the dinosaur bearing-horizons), with larger sampling of c.10 kg of the dark grey marly level of Cañalatorre fossil site which is rich in charophytes; (5) palaeomagnetic analysis of the samples collected in La Cañadilla, Fortanete, and Allueva formations; and (6) review and integration of data sets updating the stratigraphic and palaeogeographic evolution of the northeast Iberia during the latest Cretaceous.

A composite log including the best outcropping sections was used to complete a continuous sampling for the magnetostratigraphic analysis: the Fonfría log F (Fig. 3B) for the La Cañadilla Fm, the Bea log B1 (Fig. 3C) for the Fortanete Fm and for the lower levels of the Allueva Fm, and the Allueva logs A2 and A3 (Fig. 3B) for the middle and upper levels of the Allueva Fm. The Segura de los Baños log SB2 (Fig. 3A) provided additional samples for the upper part of the Allueva Fm. For the magnetostratigraphic study 117 levels were sampled, 18 from limestones of La Cañadilla Fm, 8 from limestones of Fortanete Fm, and 91 in siliciclastic levels (mudstones and sandstone) of the Allueva Fm. Sampled levels were established approximately every 3 m for the La Cañadilla-Fortanete formations (83 m-thick succession), and every 5 m for the Allueva Fm (640 m-thick succession). Limestone beds were sampled with a portable gas-powered and water-cooled drill and oriented in the field with a magnetic compass and an inclinometer. In the siliciclastic beds, a portable electrical water-cooled drill was used, also oriented in situ. The gas-powered drill provided 1–2 standard-sized samples per level, whereas the electrical drill provided 2–3 samples. Mudstone samples were easily disaggregated, so they were consolidated with sodium silicate dissolved in distilled water. A denser mixture was used to stick broken limestones back together. Once hardened, each sample was sectioned with a disc cutter, providing 2–3 measurable specimens per sample.

Both Thermal (Th) and alternating field (AF) demagnetizations were

Table 1
Key information on the newly defined Allueva Fm.

Name	Allueva Fm
Main lithology	A siliciclastic-dominated succession (mudstones, sandstones, conglomerates), with thick intervals of reddish mudstones including interbedded cross-bedded and massive-bioturbated sandstones. In the middle-upper part of the unit there are intervals dominated by well-cemented conglomerates with calcareous pebbles, that grades laterally to a carbonate dominated-succession (bioturbated marls, micrites, oncolitic and tufa limestones). Some discontinuous gypsum levels are locally found towards the middle-upper part of the unit.
Stratotype	Located around 2 km east of Allueva village is the 700 m-thick succession described in this work. *Bottom*: 40°59′02.0"N 1°01′40.2"W; *Top*: 40°58′09.4"N 1°01′12.6"W
Other type-localities	Other type-locality in the Montalbán subbasin are found near de villages of Segura de los Baños and Bea (see description in this work).
Thickness and equivalences to previous units	The overall thickness of the unit is variable (500–700 m) across the continuous exposure in the northwestern areas of the Montalbán subbasin. In the southern part of the basin (south of Martín del Río) the unit is c.300 m-thick. The lower part of the Allueva Fm consists of a 300–500 m-thick terrigenous succession and corresponds to the tecto-sedimentary unit M1 described by Pérez et al. (1983) and Casas et al. (2000). The upper part of the Allueva Fm is up to 200 m thick and is equivalent to the lower part of the tecto-sedimentary unit M2.
Boundaries	*Lower boundary:* well-marked lithological change with the thick bedded limestones of the Fortanete Fm. *Upper boundary:* Low-angle erosive unconformity with the overlying Paleogene (Eocene?) continental successions of terrigenous and carbonates.
Geographical distribution and lateral equivalences (Maestrazgo domain)	The Allueva Fm has been studied and defined in the Montalbán subbasin (northern Maestrazgo domain in the northeastern Iberian basin). The unit is also found in the nearby Aliaga subbasin. There, the A1 unit of González and Guimer (1993) equivalent to the Allueva Fm consist of a c.300 m-thick coarsening upward terrigenous dominated-succession, including scarce dinosaur remains in the upper part (Canudo et al., 2005). Southwards, in the core of a large syncline structure (i.e. Fortanete syncline), a c.50 m-thick fine-terrigenous succession with abundant latest Cretaceous charophytes (Gautier, 1980) is also regarded as equivalent to the Allueva Fm.
Depositional environment	Alluvial fans to braided distributary channel systems with development of large muddy floodplains, with local setting of lacustrine-palustrine carbonate environments.
Age Range	Middle Campanian-earliest Maastrichtian

done in Centres Científics i Tecnològics of the University of Barcelona. For AF demagnetization an AF Demagnetizer D-Tech 2000 was used in 12 limestone samples (all AF up to 200 mT in 12 measurements from 5 mT). All other samples were demagnetized using a Superconducting rock magnetometer 2G SRM 755R, a Thermal demagnetizer ASC TD48EU furnace was used to achieve the different temperature-steps used for demagnetization. Magnetic susceptibility was measured using a Kappabridge KLY-2 for all temperature-steps. Limestones samples measured using Th were heated up to 330–480 °C, and siliciclastics samples were heated up to 530–670 °C. Principal component analysis (Kirschvink, 1980) was done using Remasoft software (Chadima and Hrouda, 2006). Virtual Geomagnetic Poles (VGPs) were calculated considering the palaeomagnetic directions regarded as primary.

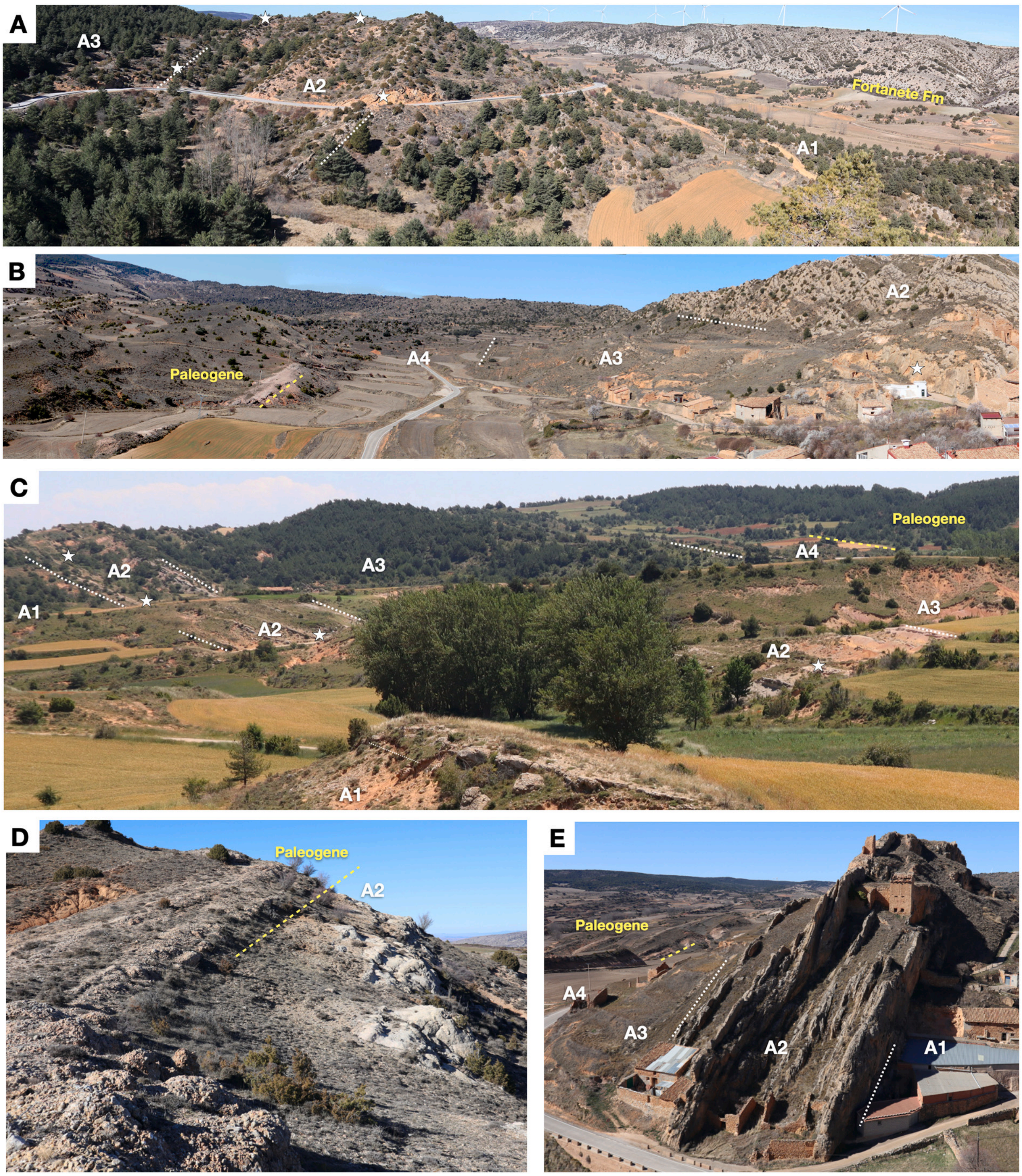

Fig. 4. **A:** Distribution of units A1-A3 in the Allueva Fm in its type locality, around the Log A2. There is a conformable boundary between the carbonates of the Fortanete Fm (to the right) and A1 unit. White stars in A, B and C indicates the location of fossil sites. **B:** Distribution of units A2-A4 in the upper Allueva Fm close to Segura de los Baños showing also the unconformity with the Paelogene unit. **C:** Distribution of the units A1-A4 in the Allueva Fm south to Allueva. **D:** Angular erosive unconformity between the whitish limestones of the Allueva Fm (A2 unit) and the Paleogene conglomerates, west to Fonfría. **E:** The conglomerates and sandstones of A2 unit forms a prominent crest around the Segura de los Baños village. The boundary between A1 and A2 units was used to define the boundary between TSUs M1 and M2 (Pérez et al., 1983; Casas et al., 2000).

4. Geological mapping: distribution and boundaries of the Allueva formation

Across the study area, the lacustrine-palustrine continental carbonates of the 20–30 m-thick Fortanete Fm are abruptly overlain by the basal levels of red mudstones and sandstones of the Allueva Fm (boundary 1 in Fig. 3). Despite this abrupt lithological change, there is a conformable boundary between both units, with only local evidence of low-amplitude erosive scours on top of the Fortanete Fm. The 500–700 m-thick Allueva Fm has been divided in four mapping units (see A1 to A4 in Fig. 2B). The distribution of these units is well observed in the continuous outcrop that extends from Allueva to Segura de los Baños villages (Figs. 4A, B, C). However, west to Fonfría only the A1 and A2 units have been mapped, because the upper A3 and A4 units are absent due to erosion previous to the sedimentation of the overlain Paleogene unit (Fig. 4D).

The unit A1 or *lower Allueva Fm* (equivalent to the TSU-M1 of Casas et al., 2000) is dominated by red mudstones with interbedded levels of bioturbated and cross-bedded sandstones, and scarce conglomeratic beds. The thickness is variable, with maximum around 500 m near Allueva, and a minimum around 300 m near Segura de los Baños. The upper boundary of the A1 unit is a conformable surface (see boundary 2 between in Fig. 3) marked locally by an abrupt vertical lithological change with the overlying A2 unit.

The *upper Allueva Fm* (equivalent to the lower part of the TSU-M2 of Casas et al., 2000) includes the A2-A3-A4 mapping units. The A2 unit consists of well-cemented conglomeratic to cross-bedded sandstone levels with red mudstone interbeds in the eastern area (Fig. 4E), which progressively grades to the marls and micritic-oncolitic-tufa limestones that dominates the central and eastern areas (Fig. 4C, D). The overall thickness of the A2 unit is relatively constant across the study area, ranging from 50 to 70 m. The unit includes most of the vertebrate fossil sites found in the central study area between the Allueva and Fonfría villages.

The boundaries between A2-A3 and A3-A4 units are conformable surfaces marked by gradual lithological changes (see boundaries 3 and 4 in Fig. 3). Units A3 and A4 are only preserved in the eastern area located between Segura de los Baños and Allueva. The A3 unit is formed by a c. 90 m-thick mudstone-dominated succession with intercalation of cross-bedded to bioturbated sandstones, and includes the vertebrate fossil sites found near Salcedillo village. The unit A4 is a c. 50 m-thick succession of poorly exposed red mudstones and scarce interbedded cross-bedded and bioturbated sandstones. No vertebrate fossil sites have been found in this unit.

The upper boundary of the Allueva Fm is a low-angle erosive unconformity across the study area (see boundary 5 in Fig. 3). This unconformity is overlain by the conglomerates, mudstones and palustrine-lacustrine carbonates of the middle and upper part of the TSU-M2, assigned in Casas et al. (2000) to the middle-late Eocene (see *Paleogene unit* in Fig. 3). In the eastern area between Segura de los Baños and Allueva, the lower part of the *Paleogene unit* is dominated by white to reddish mudstones and conglomerates with quartzitic pebbles, grading upwards to carbonates with abundant vertical root traces. West to Fonfría the lower levels of the *Paleogene unit* consist of calcareous-dominated conglomerates, red clays and interbedded limestones (Fig. 4D). The upper boundary of the *Paleogene unit* is the angular unconformity well exposed south of Segura de los Baños. This unconformity is overlain by the upper Oligocene–lowermost Miocene TSU-M4 (Pérez et al., 1983; Casas et al., 2000).

5. Charophytes from the Allueva formation: biostratigraphic remarks

The microfossil sampling of a dark grey marly interval found in the Cañalatorre fossil site (Allueva Fm, lower A2 unit, see Clt site in Fig. 3B for location) has provided a highly diverse charophyte assemblage. Up to 7 species have been found belonging to genera *Microchara, Bysmochara, Strobilochara, Nitellopsis,* and *Lychnothamnus (Pseudoharrisichara)*. From the biostratigraphic viewpoint three species stand out, *Bysmochara conquensis, Strobilochara* cf. *diademata,* and *Peckichara cristatella*.

Bysmochara conquensis GRAMBAST et GUTIÉRREZ 1977 (Fig. 5A-C) shows medium to large gyrogonites, oblate to subspherical in shape, 600–808 µm high and 656–826 µm wide, with an average isopolarity index (100 x height/width) of 98, showing usually 8 turns of the convex spiral cells in lateral view. The apex is rounded and shows a well-marked periapical thinning of the spiral cells. The base is flat and displays a large basal plate visible from the outside. The population studied in Cañalatorre shows intermediate characters between *B. conquensis* and *Bysmochara roblesii* GRAMBAST et GUTIÉRREZ 1977, particularly in the limited calcification of the apical rosette. This is the most abundant species of the assemblage.

Strobilochara cf. *diademata* GRAMBAST et GUTIÉRREZ 1977 (Fig. 5D-F) shows small to medium gyrogonites, oval subprolate in shape, 370–456 µm high and 313–373 µm wide, with an average isopolarity index of 119. The spiral cells are flat or concave and display a characteristic ornamentation made of round tubercules, which are unequally distributed. Up to 8 turns are visible in lateral view. The apex is rounded, devoid of tubercules, and without any periapical modification. The base is tapering to pointed and shows a small pentagonal basal pore. These gyrogonites are >200 µm smaller than those from the type population, from which they also differ by the absence of nodules forming a periapical "crown".

Peckichara cristatella GRAMBAST et GUTIÉRREZ 1977 (Fig. 5G-H) shows small to medium gyrogonites, subspherical to barrel-shaped, in average 446 µm high and 455 µm wide, with an isopolarity index of 98. Spiral cells display 7–8 turns in lateral view of the gyrogonite. They are characteristically ornamented with a prominent, slightly nodular mid-cellular crest, as wide as half the width of the spiral cell. The apex is rounded and spiral cells display a well-marked periapical thinning and a slight periapical narrowing to end with well-developed apical tubercules. The base is rounded to flat and shows a small pentagonal basal pore.

These three species of charophytes were first described from the Villalba de la Sierra and Sierra Perenchiza formations of the South Iberian domain of the Iberian basin, in the Cuenca and València provinces by Grambast and Gutiérrez (1977). The two formations are lateral equivalents and have been regarded as Campanian-earliest Maastrichtian in age (see Martín-Chivelet et al., 2019a, and references therein). Gutiérrez and Robles (1976) tentatively attributed the base of the charophyte-bearing formations from Cuenca and València to the early Campanian, based on a similar charophyte assemblage found near Sierra Perenchiza (València province), overlying or intercalated with the marine beds of the Sierra de Utiel Fm containing *Lacazina elongata*, a large foraminifer belonging to the latest Santonian. In turn, the top of the charophyte-bearing beds from that area was placed at the base of late Maastrichtian by the occurrence of dinosaur eggshells from that age at Barranco de la Hoz (Cuenca province), in the same sample that contained some of the charophytes described here.

Peyrot et al. (2013, 2020) studied the palynology from the charophyte-bearing beds of the Villalba de la Sierrra and Sierra Perenchiza formations (south Iberian domain) and ranged the pollen and spores in the late Campanian and early Maastrichtian. Recent study of the charophytes from the Upper Cretaceous of the northern Castilian domain found that *Bysmochara conquensis* is restricted in that area to the early Maastrichtian, based on correlation with a rudist fauna (Feist and Floquet, 2022). However little detail is known from the late Campanian charophyte assemblages from the same localities, when the deposits were marine-influenced, i.e., of subtidal, intertidal or supratidal-sabkha facies (Feist and Floquet, 2022), and thus poor in charophytes. In conclusion, a late Campanian to early Maastrichtian age is so far the most probable age for the charophyte assemblage found in the upper part of the Allueva Fm.

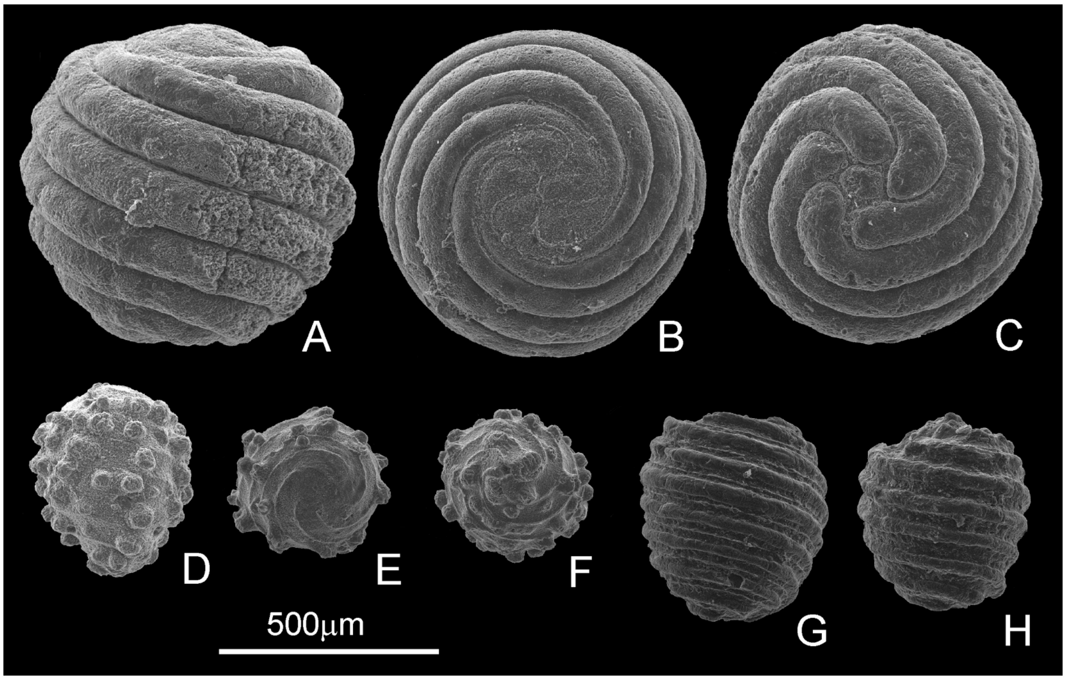

Fig. 5. Charophytes specimens from sample Clt, Cañalatorre fossil site, Allueva Fm (see Fig. 3B for location in the middle part of the A2 unit). **A-C:** *Bysmochara conquensis*, A lateral view, B apical view, C basal view (MPZ 2022/918-921-922); **D-F:** *Strobilochara* cf. *diademata*, D lateral view, E apical view, F basal view (MPZ 2022/919923-924); **G-H**: *Peckichara cristatella*, G lateral view, H lateral view (MPZ 2022/920-925).

6. Paleomagnetic results: age constrains for the Allueva formation

6.1. Paleomagnetic components and stability

As explained above (section 3), a composite log was used to complete a continuous sampling of La Cañadilla, Fortanete and Allueva formations for the magnetostratigraphic analysis. A total of 27 limestone and 90 redbeds (mudstone and sandstone) samples were thermally demagnetized, from which the characteristic component could be isolated in 16 and 63 samples, respectively. The natural remanent magnetization (NRM) in the limestones presents a mean value of 0.12 mA/A and a standard deviation of 0.16 mA/m, while the red layers present higher intensities, with a mean NRM of 4.28 mA/m and a standard deviation of 25.25 mA/m (Fig. 6A).

In order to filter the results, the isolated paleomagnetic components are divided into four different classes, from highest to lowest quality from Class 1 to Class 4. Class 1 is outlined as a well-defined component going towards the origin (without forcing it to pass through the same). Class 2 shows a well-defined component with a tendency to go towards the origin, but because it has a noisy signal it is forced to pass through the origin. On the contrary, class 3 shows a well-defined paleomagnetic component, but it does not pass through the origin and could have a higher temperature component that cannot be isolated. Finally, class 4 is defined as a cluster that cannot be demagnetized and is assumed to be the characteristic component (ChRM) and is therefore forced towards the origin.

Limestones are very weak magnetically and quite unstable during heating. In general, Class 4 dominates, and between 200 and 450 °C the magnetization of the sample hardly varies. Despite their low intensity, the directions are repeated in each of the demagnetization steps, generating a clustering that is rather credible for calculating the ChRM (Fig. 6B), up to 400–450 °C, and after that spurious components appear due to the neoformation of ferromagnetic *s.l.* minerals during heating. Moreover, due to the directions obtained, they will result in reasonable Virtual Geomagnetic Poles (VGP). On the other hand, red beds show a more heterogeneous behavior and generally higher paleomagnetic quality (Fig. 7). Of the 65 ChRM isolated, 23 correspond to Class 1, 19 to Class 2, 18 to Class 3 and 5 to Class 4.

The Class 1 samples show intensities on the order of 1 mA/m, and the ChRM can be isolated in an unblocking temperature spectrum around 400–600 °C. Class 2 samples are similar to the previous ones, but are usually weaker (0.1–0.2 mA/m), generating more noise in the magnetic signal, and therefore they are forced to pass through the origin when calculating the ChRM. Class 3 samples have intermediated intensities, of the order of 0.5 mA/m. Occasionally, as is the case with sample AM07-01B, they are characterized by a noisy signal in which a paleomagnetic component between approximately 250–400 °C can be observed, which although it does not go to the origin, no other higher temperature component is evident. At other times, as in AM40, a well-defined paleomagnetic component is observed between 300 and 500 °C which, although it does not go to the origin, a component of higher temperature is not observed either. On the contrary, sometimes in some samples a paleomagnetic component is observed between 300 and 550 °C, but it does not go to the origin, and if the Greatest Circles are analyzed, it seems that the directions in the demagnetization diagram were to quadrants of opposite polarity to the observed component; in these cases, no paleomagnetic component has been calculated. Finally, some samples do not show a well-deployed paleomagnetic component, but a clustering of data can be observed and the paleomagnetic component can be calculated by forcing it to pass through the origin. In most cases, it has not been heated above 610 °C because the samples become unstable due to mineralogical neoformation above this temperature.

The sampled profiles constitute a monocline making it impossible to perform the fold test. However, it is observed that the characteristic component has an antipodal character (Fig. 8). The reversal test (Tauxe, 2010) shows that the normal and reverse mean directions share a common true mean, showing inclinations close to what is expected for the Upper Cretaceous rocks of Iberia (Dec: 354°, Inc.: 42°; Osete et al., 2006; Neres et al., 2012). The antipodality observed after bedding correction (ABC), as well as the observation of normal and inverse polarities with similar paleomagnetic behavior, allow considering the

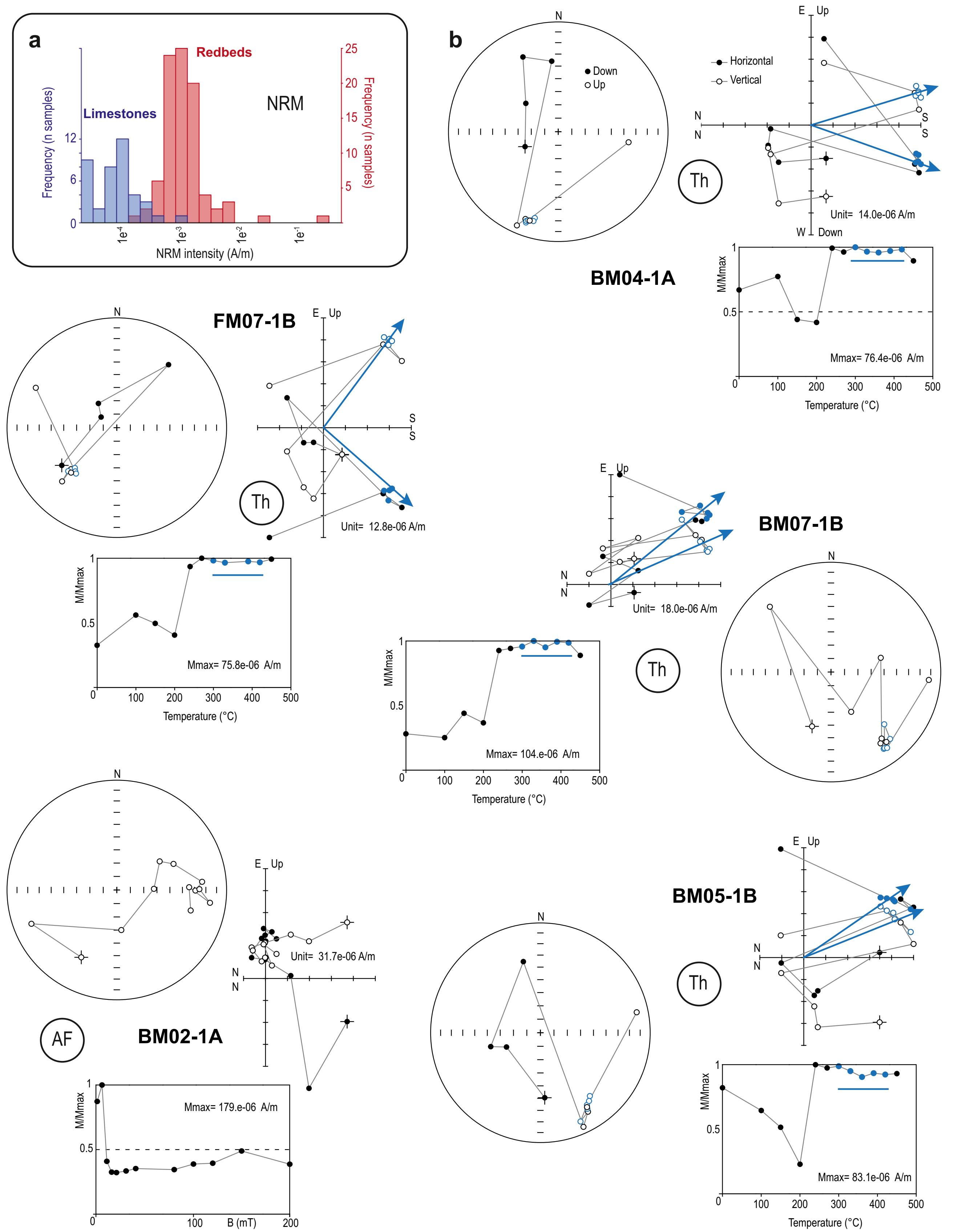

Fig. 6. **A:** Histogram showing the intensity of natural remanent magnetization (NRM) for limestones and redbeds. **B:** Thermal (Th) and alternating field (AF) stepwise demagnetization of the NRM for representative samples of Class 4 limestones, showing for each sample the othogonal plot, the equal área projection and the intensity decays curves. All plots are in stratigraphic coordinates.

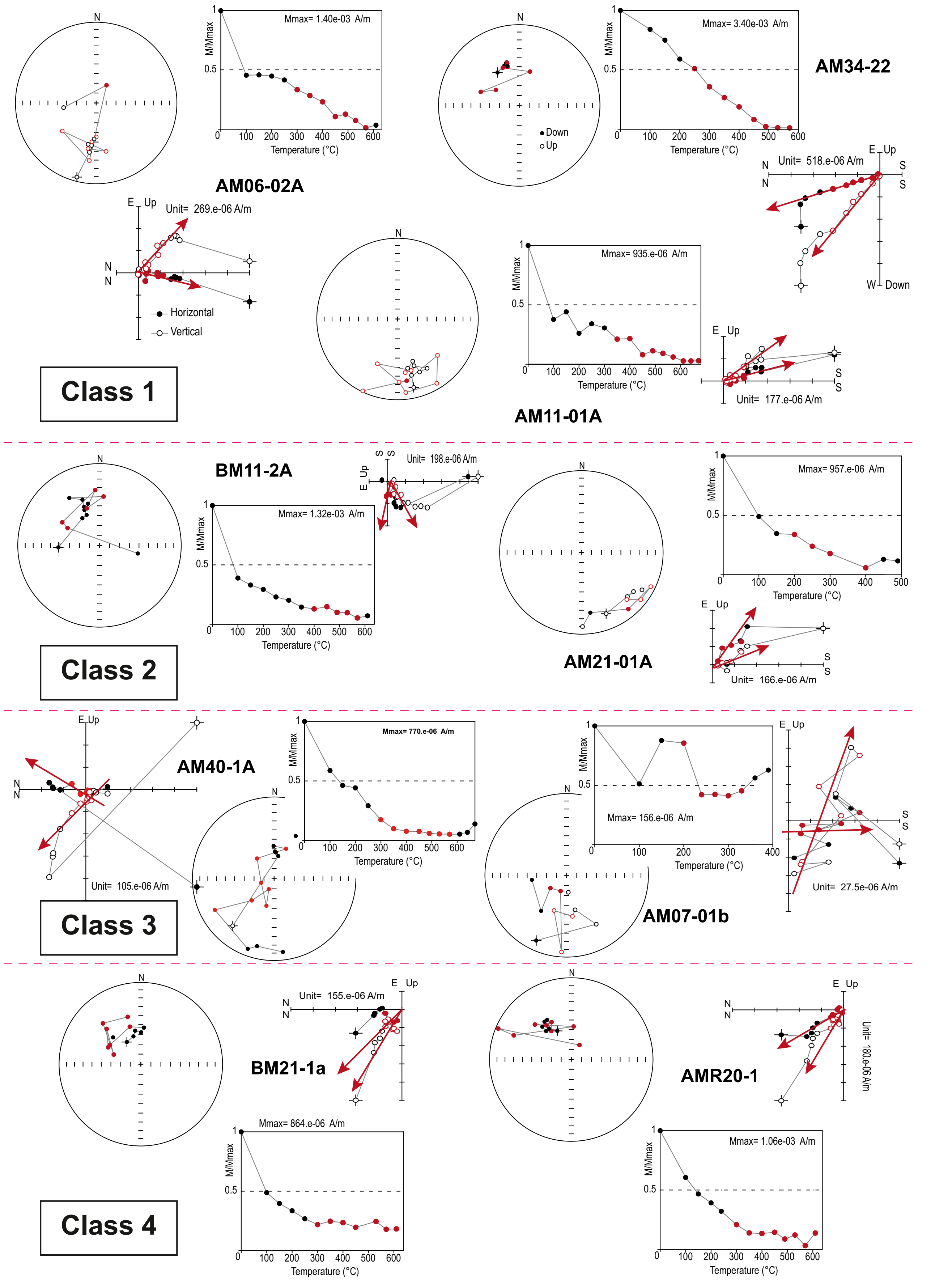

Fig. 7. Thermal stepwise demagnetization of the NRM showing the different behavious and clases observed in redbeds. All plots are in stratigraphic coordinates.

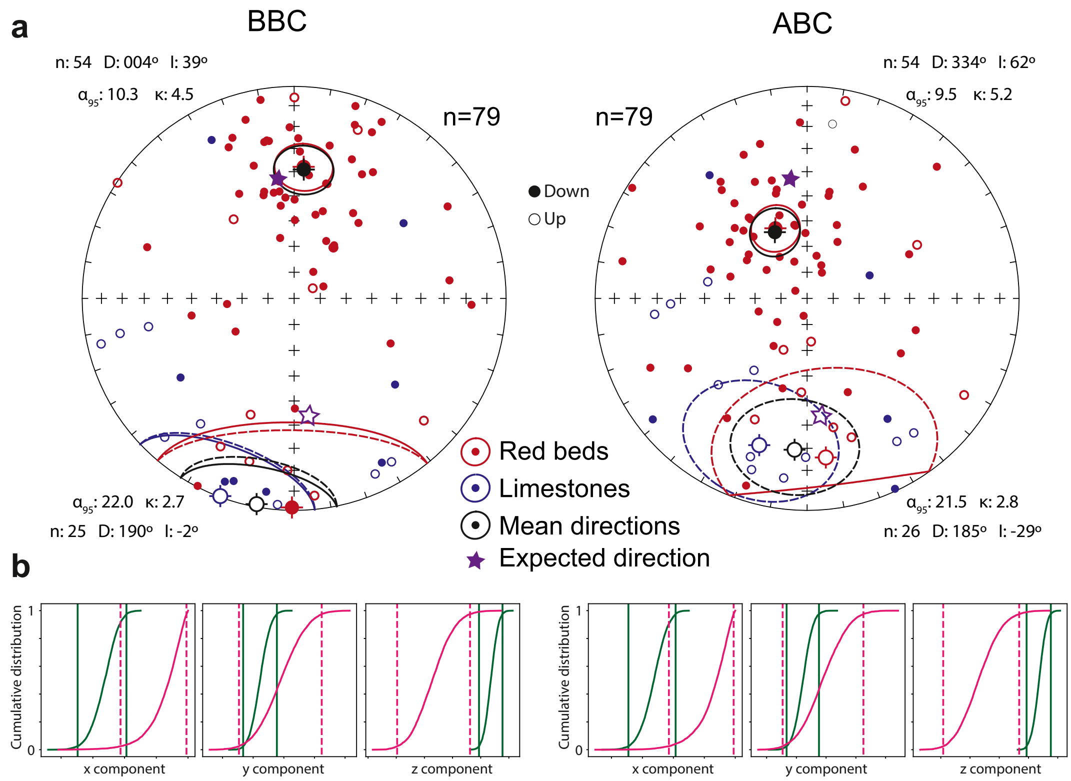

Fig. 8. A: Directions of the isolated characteristic remagentization and normal and reversed mean directions, before and after bedding correction (BBC and ABC respectively). **B:** Reversal test (Tauxe et al., 2016) showing an overlap between both mean directions both in the x and y component but not in the z component.

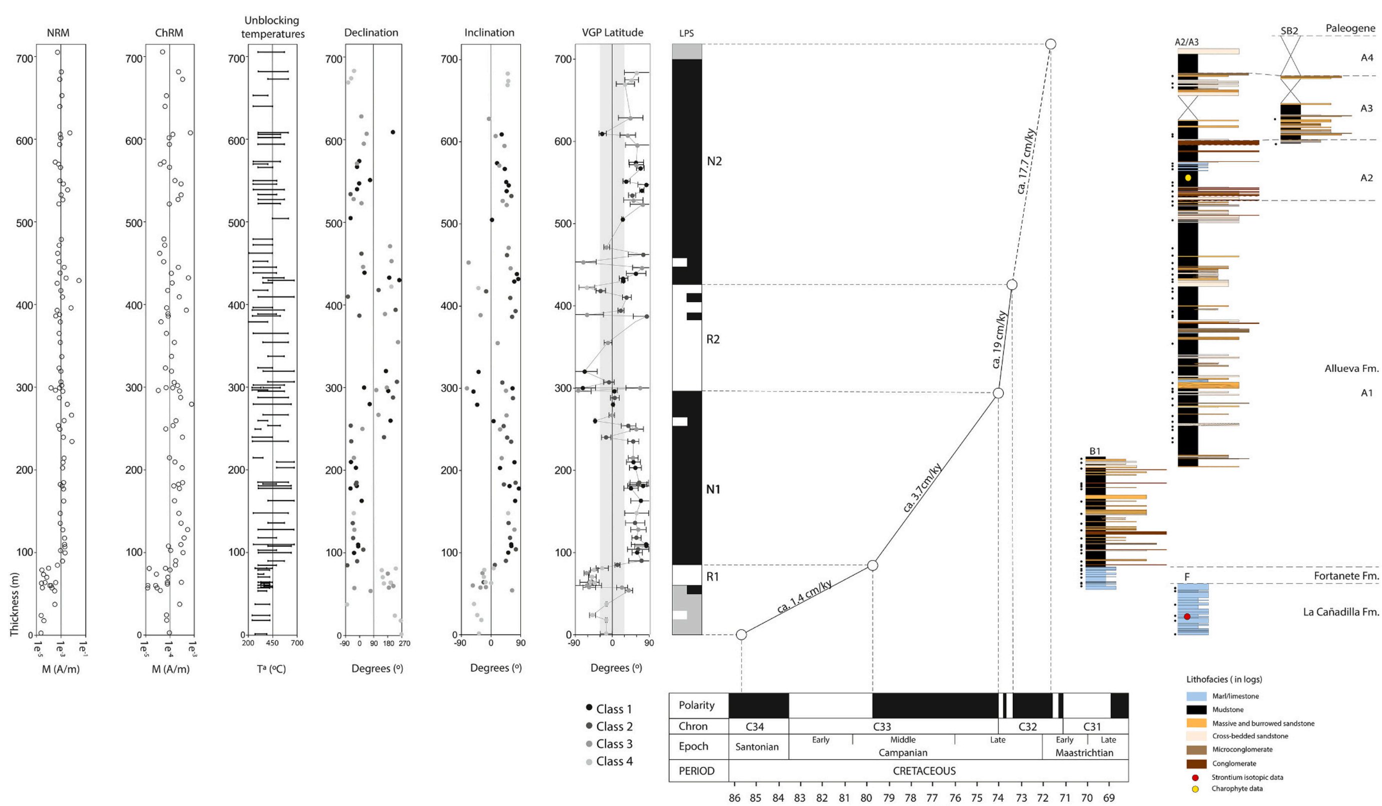

Fig. 9. To the left is the synthetic representation of the composite log including the Fonfría (log F), Bea (log B1), Allueva (logs A2/A3), and Segura de los Baños (log SB2) sections analyzed to develop the local polarity sequence (LPS). The proposed correlation with the global polarity time scale (Ogg, 2012; Haq, 2014) allow to estimate sedimentation rates for the successive subchrons. NRM: natural remanent magnetization, ChRM, characteristic remanent magnetization, VGP, virtual geomagentic poles**.** The four defined paleomagnetic classes are differentiated by colors from lightest to darkest (classes 4 to 1).

primary behavior of the characteristic component.

6.2. Local polarity sequence and correlation to the Global Polarity Time Scale

From characteristic paleomagnetic directions with maximum angular deviation <25°, Virtual Paleomagnetic Directions (VGP) and associated dm uncertainty parameters were calculated (e.g. Butler, 1992), and a cutoff of 30° (Vandamme, 1994) for the VGP latitude was applied. Despite the moderate quality of the paleomagnetic signal, these criteria help to eliminate noise and uncertainty to establish a local magnetostratigraphic framework (Fig. 9).

The Local Polarity Sequence (LPS) has been confidently stablished for most of the studied succession except for the lowermost and uppermost levels (see grey intervals in Fig. 9). The base of the sequence (0–58 m) composed by limestones beds of La Cañadilla Fm presents much uncertainty so that no magnetozone is established for it. Moreover, the uppermost part of the Allueva Fm (A4 unit) is poorly exposed and could not be confidently sampled. However, most of the Fortanete Fm, shows in general qualities of class 3 and 4, but a consistency among the data allows establishing the inverse zone R1. Coinciding with the boundary between the Fortanete to Allueva formations, there is a change of paleomagnetic behavior, appearing better paleomagnetic qualities (classes 1 and 2), as well as a change of polarity. The lower 170 m of the Allueva Fm (83–253 m) show normal polarities in a homogeneous way, allowing to define the normal zone N1. Between meters 259 to 450, the directions obtained are less homogeneous. Although inverse polarities dominate, there are some samples of intermediate quality showing normal polarity. After the slightly heterogeneous transit around 450 m, the behavior is again homogeneous and with good paleomagnetic qualities, defining the last normal polarity zone N2 in the upper part of the succession (418–723 m).

There are some available data that allow to constrain the correlation of the Local Polarity Sequence (LPS) with the Global Polarity Time Scale (GPTS) (Ogg, 2012). As explained above, the Santonian age for most of La Cañadilla Fm is well-stablished (Martín-Chivelet et al., 2019a; Torromé et al., 2022). In our case, we have not been able to define the polarity zone at the base of the sequence due to the poor quality of the paleomagnetic signal, but since the Santonian is related to the chron C34n, the base will correspond to that chron (Fig. 9). Moreover, in coherence to previous age assignments (e.g. Floquet, 1991; Martín-Chivelet et al., 2019a; Torromé et al., 2022) the paleomagnetic data indicates that the Santonian-Campanian boundary (i.e. boundary between chrons C34 and C35) is located around the boundary between La Cañadilla and Fortanete formations.

On the other hand, the analysis of charophytes obtained from the Cañalatorre fossil site at meter 525 of the composite magentostratigraphic log (i.e. middle part of the N2 zone of the LPS) indicates a late Campanian-early Maastrichian age (see section 5). Considering this age constrain, the correlation between LPS and GPTS allows us to define more precisely age of the Allueva Fm, as well as the variations in the sedimentation rate for the different sections of the series.

The LPS presented here shows a good correlation with the Campanian-earliest Maastrichtian GPTS (Fig. 9). This time interval of the GPTS is composed of two groups of chrons, C33 and C32. The C33 starts with the reverse polarity chron C33r for the first 3.7 Ma, leading to the normal polarity chron C33n lasting about 5.6 Ma. On the other hand, the C32 group is more complex, starting with the chron C32r that is composed by three subchrons of shorter duration of 1 Ma (C32r.2r, C32n.1n and C32r.1r) followed later by the 1.6 Ma chron C32n and spanning the latest Campanian-earliest Maastrichtian. The LPS presents alternately, from base to top, two inverse zones R1 and R2 and two normal zones N1 and N2. On the other hand, within the inverse interval composed by R2, a normal zone could be present around 400 m. Therefore, the four main zones defined in the LPS correlate well with the four presents in the GPTS, with the presence in addition of the short-lived subchron C32r.1n of about 0.05 Ma.

According to the above exposed data and interpretations, it is concluded that the Fortanete Fm is mostly early Campanian in age, whereas the Allueva Fm was mostly deposited during the middle-late Campanian (Fig. 9). The lower 170 m of the Allueva Fm were deposited during the subchron C33n, at an average compacted sedimentation rates of c.4 cm/ky. A sharp increase of compacted sedimentation rates occurred onwards from the middle part of the late Campanian (i.e. boundary between chrons C33 to C32), with rates of c.17–19 cm/ky during subchrons C33r and C34n.

7. Facies analysis: sedimentological remarks

The middle-upper Campanian Allueva Fm includes a wide spectrum of laterally and vertically related lithofacies, including mudstones, gypsum, carbonates (marls and limestones), sandstones (massive, bioturbated, and cross-bedded) and conglomerates. The correlation of the studied logs near the localities of Segura de los Baños, Allueva, and Bea show the overall lateral and vertical distribution of the identified facies associations in an along-strike section that runs almost parallel to the marginal uplifted area represented by the southern flank of the Montalbán anticline (Fig. 10). The overall facies distribution shows a poorly-defined coarsening to finning upward evolution, with larger concentration of the conglomeratic beds around A2 unit.

Pérez et al. (1983) studied the Allueva Fm in the entire Montalbán subbasin, and concluded that its deposition took place in a complex alluvial system. In the along-strike section reconstructed here, only the medium and distal areas of this alluvial system are observed. Key information and interpretation of the five facies associations (FA1–FA5) identified in the Allueva Fm is provided below.

Facies association 1 (FA1) is characterized by the common presence of conglomerate levels, and is found in few intervals in the A1 and A2 units (Fig. 10). Conglomerates are clast-supported and relatively poorly-sorted, and are dominated by well-rounded and calcareous pebbles (Fig. 11A). Dinosaur bones may locally appear reworked. There are some gravelly levels arranged in relatively continuous irregular tabular beds. However, most of the conglomerates form discontinuous (lenticular and channelized) levels up to 1–5 m-thick interfingered with cross-bedded gravel beds and sandstones (Fig. 11B), which stack to well-cemented discontinuous intervals up to 10–15 m-thick (Fig. 11C). Scour structures eroding the interbedded meter-thick red mudstones are also common (Fig. 11D). The observed geometry and internal architecture indicate that sedimentation of FA1 took place in a complex braided distributary system that was laterally heterogeneous (Pérez et al., 1983; Nichols and Fisher, 2007). Most conglomeratic levels would represent channel bars, while cross-bedded granule beds and sandstones indicates sedimentation in channels by accretion of bars and migration of bedforms such as dunes or megaripples (Allen, 1983; Huerta et al., 2011). The tabular gravelly levels are similar to conglomerate sheet-like channel bodies described as parts of a distributive fluvial system and interpreted as laterally stacked channel belt fills (Huerta et al., 2011). Within these stacks of conglomerate, it can be difficult to identify the scour surfaces that mark the base of a channel and hence recognise individual channel-fill succesions (Nichols, 2005). Alternatively, sheets of conglomerates in braided fluvial systems have been interpreted as longitudinal bars, commonly representing multistorey deposition shown by multiple scoured surfaces or interbedding of thin sandstones (e.g. Ramos and Sopeña, 1983). The flood plain related to these conglomeratic-sandy distributary channel systems would result in the sedimentation of fine terrigenous deposits after major flooding events, represented by the interbedded red mudstone lithofacies (Fig. 11D). The measured palaeocurrent data with dominant migration of bars towards the SW–S (see Fig. 6B and Pérez et al., 1983) indicates that this braided system was sourced from nearby uplifted areas located to the north-northeast.

Facies association 2 (FA2) is dominated by sandstones and fine-gravel beds alternating with red mudstones. Cross-bedded sandstones and

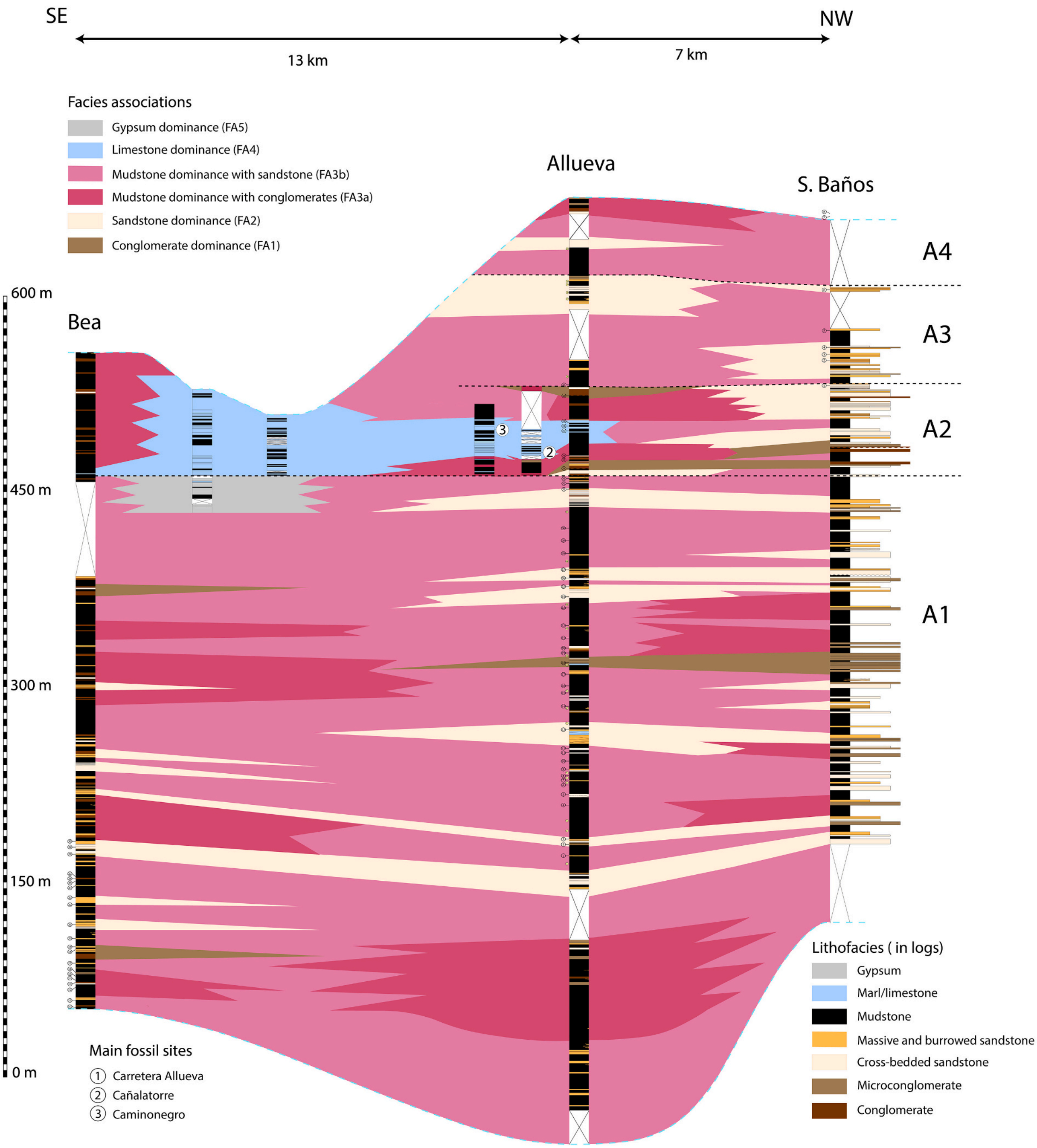

Fig. 10. Overall distribution of facies association FA1 to FA5 in the Allueva Fm after correlation of the Bea, Allueva and Segura de los Baños logs (see Fig. 3 for location). The vertical succession of lithofacies in logs is indicated in a different key colour. Increments in the left composite vertical scale is 5 m. Small numbers in the left part of the columns locate the beds sampled for paleomagnetic analysis.

conglomerates form discontinuous lenticular levels of variable thickness ranging from few dm- to up to 7 m-thick. The grain size is variable, mostly medium to coarse sandstones, with common presence of dispersed soft and calcareous/quartzite pebbles (Fig. 11E). Graded successions with accumulation of conglomeratic levels at the bottom of the cross-bedded sets (planar and though cross-stratification) are common. There are some deposits of well-sorted cross-bedded sandstones with pin-stripe lamination and contorted bedding (Fig. 11F). FA2 also includes dm- to m-thick reddish to greyish massive and bioturbated fine to coarse sandstones with variable lateral extent and geometry (from tabular to lenticular). The presence of intense burrowing (mostly *Taenidium* traces c.1–2 cm in diameter) on top of these sandstones is also common (Fig. 11G). FA2 mostly represent the sedimentation after the migration of bars in a sandy braided distributary system (Pérez et al., 1983). The presence of reactivation surfaces within the cross bedded intervals indicates the episodic subaerial exposure of the fluvial bars. Well-sorted cross-bedded sandstones showing pin-stripe lamination can be related to the local development of eolian dunes (Fryberger and Schenk, 1988). The presence of convoluted bedding can be also explained as water is squeezed out of sediment in front of an advancing dune (Collinson and Mountney, 2019). The eolian reworking of the alluvial plain in braided distributary systems is well documented and related to phases of relative aridity (e.g. Nichols, 2005). Tabular to lenticular commonly-bioturbated sandstone beds are related to deposition in the flood plain after major flooding events (crevasse splay deposits) or in abandoned channels, which are eventually colonized by

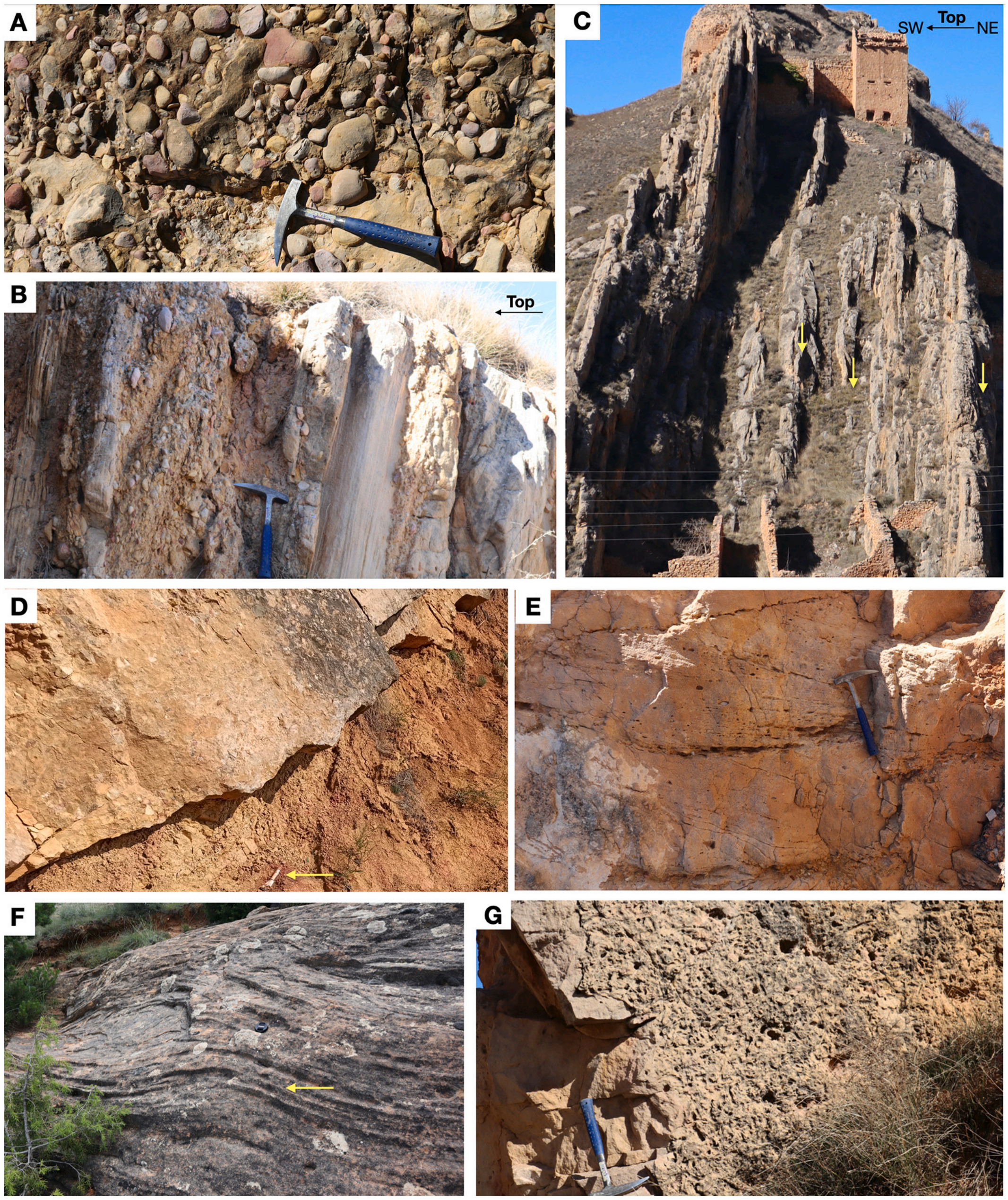

Fig. 11. **A:** Aspect of the conglomerates of facies association 1 (FA1), which are generally dominated by calcareous pebbles. **B:** Interfingering of conglomerates and cross-bedded sandstones in FA1. **C:** The A2 unit in Segura de los Baños is dominated by the FA1/2; notice the presence of cross-bedded sandstones and conglomerates (yellow arrows) in lenticular levels showing southwards migration of bedforms. **D:** Scours at the base of conglomerates (FA1) overlaying reddish mudstones with well-preserved dinosaur bones (Carretera de Allueva site, the yellow arrow point to a 15 cm-long dinosaur bone). **E:** Cross-bedded coarse sandstones with soft pebbles. **F**: View of the cross-bedded sandstones with contorted bedding and pin-stripe lamination interpreted as eolian dunes (FA2). **G:** Top of a coarse sandstone bed highly bioturbated by invertebrates attributed to *Taenidium* traces (FA2). (For interpretation of the references to colour in this figure legend, the reader is referred to the web version of this article.)

invertebrate fauna (Miall, 1977; Nichols and Fisher, 2007). The common occurrence of red mudstone lithofacies are related to fine-grained overbank deposits in the flood plain of the braided system.

Facies association 3 (FA3) is dominated by the mudstone lithofacies. These mostly consists of decametre-thick light brown to reddish intervals, either massive or with scarce bioturbation (Fig. 12A). Fossil content in the reddish mudstones is scarce, but exceptionally they include well-preserved dinosaur bones (*Carretera Allueva fossil site*, Fig. 11D). Some mudstone and marly intervals also display brown, red and greyish colors with hydromorphic features, with the occasional presence of levels with ferruginous ooids and pisoids. There are also present discontinuous levels of metre-thick dark grey mudstones and marls, rich in organic matter (Fig. 12A). The dominant reddish mudstones represent fine-grained floodplain facies oxidized under subaerial exposure conditions. The occasional presence of levels with ferruginous ooids and pisoids gives further indication of soil development, as described in other Cretaceous units of the northern Iberian basin (e.g. Laita et al., 2020). The development of local, more humid floodplain areas with settlement of ponds are indicated by the presence dark grey mudstones. Two subfacies associations have been differentiated. The mudstone dominated FA3a includes the local presence of conglomeratic massive irregular beds and is concentrated in the western and eastern marginal studied areas (Fig. 10). Paleocurrent data indicates that the episodic high-energy flows (probably flash floods) giving rise these

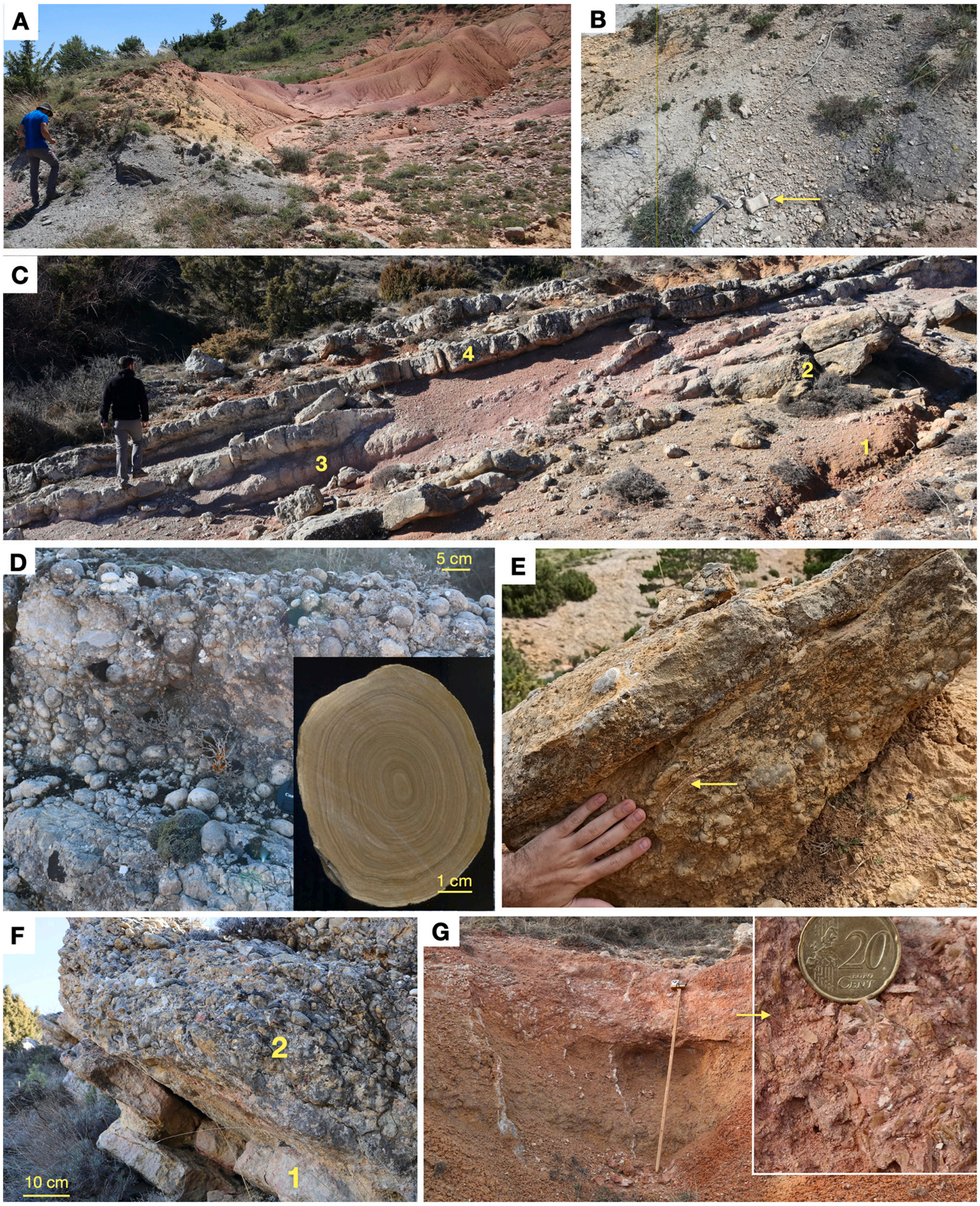

Fig. 12. A: Broad aspect of the reddish mudstones that dominate facies association 3 (FA3). The dark grey levels to the left correspond to laminated marls rich in organic matter. **B:** The grey marls with abundant organic matter of the Cañalatorre fossil site includes abundant remians of dinosaurs including caudal vertebras of titanosaur sauropods (see yellow arrow). **C:** Aspect of the FA5 south of Allueva showing a flooding sequence with red mudstones (1), channels filled by large oncolites and steam debris (2), marly limestones with vertical root traces (3), and lenticular to irregular micritic beds (4). **D:** Graded levels with oncolites up to 6 cm in diameter. The inset shows a polished slab of an oncoid, with the irregular concentric lamination. **E:** A channelized oncolitic-detrital level bearing a resedimented dinosaur bone (see yellow arrow). **F:** Micritic limestone beds (1) sharply overlain by a conglomerate bed dominated by calcareous pebbles (2). **G:** Orange mudstones capped by an interval with common mm- to cm-scale lenticular gypsum crystals (inset). Jacob bar is 1.5 m-long. (For interpretation of the references to colour in this figure legend, the reader is referred to the web version of this article.)

coarse-grain levels were sourced from the more proximal northern uplifted areas. The FA3b is characterized by the presence of interbedded levels of massive to bioturbated fine to medium sandstones, deposited in abandoned channels or in the flood plains during flooding events. Sandstones would be associated with the setting of numerous dispersed small-low flow channels (Pérez et al., 1983).

Facies association 4 (FA4) is characterized by the dominance of carbonates. Irregular, dm-thick marls and carbonate beds are found interbedded between the terrigenous facies at any level of the stratigraphic sections. However, a wide spectrum of carbonate facies occurs in a continuous interval up to 70 m-thick located between Allueva and Bea localities (A2 unit, Fig. 10). There, massive white to light grey micritic carbonates (lime mudstones and wackestones with charophytes and gastropods) form irregular to lenticular m-thick beds interbedded with greyish to pinkish poorly fossiliferous marly intervals (Fig. 12C). There are also local discontinuous dark grey marls, which include the richest fossil sites of the Allueva Fm, with abundant charophytes, gastropods, eggshell and vertebrate bone fragments (*Cañalatorre fossil site*, Fig. 12B).

The micritic and marly facies may have local development of vertical root traces. Some m-thick micritic mounds of possible microbial origin are common. Grain-supported limestones are also present, bearing abundant oncolites of several cm of diameter, along with debris of tufas and calcified stems (Fig. 12D). These levels form discontinuous dm-to m-thick lenticular to channelized beds and may include fragments of dinosaur bones (*Cordal Allueva-2 fossil site*; Fig. 12E). The FA4 represent the sedimentation in lacustrine-palustrine settings developed in the distal area of the alluvial system. Massive micritic limestones with local development of microbial mounds are interpreted as deposited in the lacustrine environment. The marginal palustrine areas are represented by the bioturbated micrites, with abundant root traces. The presence of intervals rich in tufa fragments, and the channelized levels with large oncoids indicates the presence of stream channels with water turbulence. On the other hand, the presence of small calcified stems and smaller tubular oncoids need less restrictive conditions to form, being able to develop in isolated ponds and in the main lakes when the water level is low (e.g. Alonso-Zarza and Calvo, 2000). Facies succession indicates a progressive flooding of the alluvial plain, from red lutites (FA3) deposited in the exposed flood plain, to small stream channels with oncoids, palustrine carbonates with root traces, and subaquatic lenticular micritic beds (Fig. 12C). The presence of conglomeratic levels eroding the micritic beds (Fig. 12F) represent stages of sharp progradation of the alluvial system.

Facies association 5 (FA5) has been only found on top of the A1 unit, between the Bea and Fonfría villages (Fig. 6). There, an up to 30-m thick interval dominated by red mudstones show a variable proportion of microcrystalline gypsum and dm-thick isolated levels of limestone and marls interbedded. The gypsum-rich levels form sequences up to 2–4 m-thick, with the proportion of gypsum crystals gradually increasing upwards, ending with 0.3 to 0.5 m-thick irregular beds formed almost entirely by gypsum (Fig. 12G). Gypsum-rich intervals consists of accumulation of small lenticular crystals that are embedded in mudstone matrix. This indicates evaporite precipitation within sediment in a dry mudflat to a saline mudflat under arid to semiarid condition. Similar deposits have been described recording sedimentation in a playa–lake system with an extensive development of mud flats (Hardie et al., 1978; Huerta et al., 2010). Mudstones bearing interstitial gypsum record sedimentation of the suspended load from unconfined flows, and gypsum precipitation probably occurred in areas where the groundwater table was close to the surface (Hardie et al., 1978). In this context, marls and limestones interbeded within the evaporitic mudstones represent carbonate precipitating lakes or ponds (Huerta et al., 2010).

In summary, sedimentation of the Allueva Fm occurred in the middle-distal domain of an alluvial-fluvial system sourced from the northern uplifted areas of the Montalbán anticline. The dominant lithology are reddish mudstones deposited in the exposed alluvial plains, with the ephemeral setting of ponds (dark marls) and palustrine areas (marls and limestones with root traces). Common invertebrate traces in relatively continuous sandstone beds indicate stages of stabilization in the alluvial plain. There are also evidences of local soil development (hydromorphic soils, iron ooids and pisoids). A fluvial-braided distributary channel system is also characterized, with the local formation of eolian dunes. Evidences of evaporation with gypsum precipitation are concentrated in the upper part of the A1 unit. More humid conditions with increase of water input in the alluvial system during the sedimentation of the A2 unit resulted in the setting of a large carbonate lacustrine area, with intense microbial activity (micritic mounds, oncolites).

8. Vertebrate fossil record of the Allueva formation

Table 2 summarizes the main findings in the most significant fossiliferous outcrops found in the Allueva Fm. These are located within the municipalities of Bea, Allueva, and Salcedillo, laterally spaced up to 15 km apart (Fig. 3). Most of the vertebrate fossil localities have been recently discovered and belong to A2 unit from the Allueva Fm, whereas two previously known localities (Salcedillo Clásico A and B) belong to the the A3 sequence (Fig. 2C).

Fine-grained sediments (red mudstones and grey marls) are the most frequent lithologies yielding vertebrate fossil remains. Within the facies associations described from the Allueva Fm, FA3 (mudstone dominance) and FA 4 (limestone dominance) are clearly the most fossil-rich. In these facies, the vertebrate remains are generally well-preserved indicating a very limited degree of reworking. They are commonly disarticulated and isolated bones, with a variable degree of breakage and weathering. Often the remains from some localities (e.g. Cordal Allueva 1, Gusepa, Cañalatorre, and Las Balsas) show bone surfaces involved by oncolitic covers, which would be indicative of an association between bioclastic accumulation and microbial development. Levels with high bone concentration or high taxon-diversity have not been recognized.

Based on the preservational features of remains, the most common taphonomic mode identified is that of isolated macrofossil bones. The presence of isolated bones has been reported from conglomeratic levels (distributary channel system of FA1) to alluvial floodplain (FA3) and palustrine-lacustrine (FA4) deposits. In a few cases, disarticulated bones

Table 2
Vertebrate fossil sites from the Allueva formation.

Fossil site	code	Identifiable fossil elements	Preservational features	Lithology	Allueva unit
Carretera Allueva	CA	Ornithopod sacrum and Limb bones, crocodylomorph partial dentary	Disarticulated bones, associated specimen	Red mudstones	Lower A2
Cordal Gris	CrG	Titanosaur caudal vertebra	Isolated bones	Grey marls	A2
Cordal Allueva 1	CrA1	Titanosaur caudal vertebra	Isolated and broken bones	Red mudstones	A2
Cordal Allueva 2	CrA2	Titanosaur dorsal vertebra	Isolated bones (ex situ)	Unknown	A2
Carretera Barranco (A and B)	CB	Dinosaur? bone fragments	Isolated and broken bones	conglomerates	Upper A2
Cañalatorre	Clt	A titanosaur partial caudal series (vertebrae and haemal arches)	Disarticulated bones, associated specimen, and microfossil content	Grey marls	A2
Camino Negro	CN	Undetermined bone fragments	macrofossil broken remains and microfossil content	Dark-grey marls	A2
Las Balsas (0,1,2)	Lb	Isolated dinosaur vertebra, crocodylomorph osteoderm	Isolated bones of some vertebrates	Grey Marls	A2
La Llana 2	Ll2	Dinosaur bone fragment	Isolated and broken bones	Grey Marls	A2
Gusepa (1 and 2)	G	Dinosaur limb bone fragments	Disarticulated bones	Brown mudstones	A2
Salcedillo clásico A	SCA	Dinosaur caudal vertebra and bone fragments	Disarticulated bones	Brown mudstones	A3
Salcedillo clásico B	SCB	Large-sized dinosaur bone fragment	Isolated bones	Brown mudstones	A3

of associated specimens have been identified such as in Carretera Allueva (FA3) and Cañalatorre (FA4) localities. In addittion, micropalaeontological content (i.e. microvertebrate bones, eggshells, and charophytes among others) have been recognized from the localities of Cañalatorre and Camino Negro (marly deposits, FA4). In absence of any clearly-distinguishable preservational bias, the relationships between the fossil record and the facies distribution of the Allueva Fm indicate that the more humid conditions in the alluvial system including lacustrine areas during the sedimentation of the A2 unit were favorable to support vertebrate-rich paleocommunities in this area of the Maestrazgo domain.

A first approach to the systematic analysis of the Allueva Fm vertebrate record reveals that titanosaur sauropod dinosaurs are the most frequent among the identifiable remains. Other vertebrates present in the fossil assemblage are ornithopod dinosaurs, crocodylomorphs, and testudines. Among the recovered material, 10 caudal vertebral centers of sauropod dinosaurs are the most significant fossils. These come from the sites of Cañalatorre and Cordal Gris, and are labelled with numbers MPZ-2022/571 to MPZ 2022/580 from the Museo de Ciencias Naturales de la Universidad de Zaragoza (Canudo, 2018).

The most complete vertebra MPZ 2022/571, coming from the Cordal Gris site, preserves the neural arch (Fig. 13A-C). It is a middle caudal vertebra with the neural arch anteriorly placed over the centrum, a character diagnostic of Titanosauriformes (Salgado et al., 1997). It has an elongated centrum which is fairly dorsoventrally flattened. The anterior articular face is concave whereas the posterior one is convex. This character is usually described as strongly procoelic centrum, which is characteristic in titanosaurs (Salgado et al., 1997). This vertebra lacks the cancellous bone typical of some South American titanosaurs, but it is also absent in European taxa such as *Lirainosaurus* or *Lohuecotitan* (Díez Díaz et al., 2016). The neural spine is laminar, low, and anteroposteriorly extended. The prezygapophyses are robust, with a length which is similar to that of the centrum as is seen in *Liranosaurus* (Sanz et al., 1999). The articular facets of the prezygapophyses are ventrally directed. The anterior and posterior hemapohysial facets are well developed.

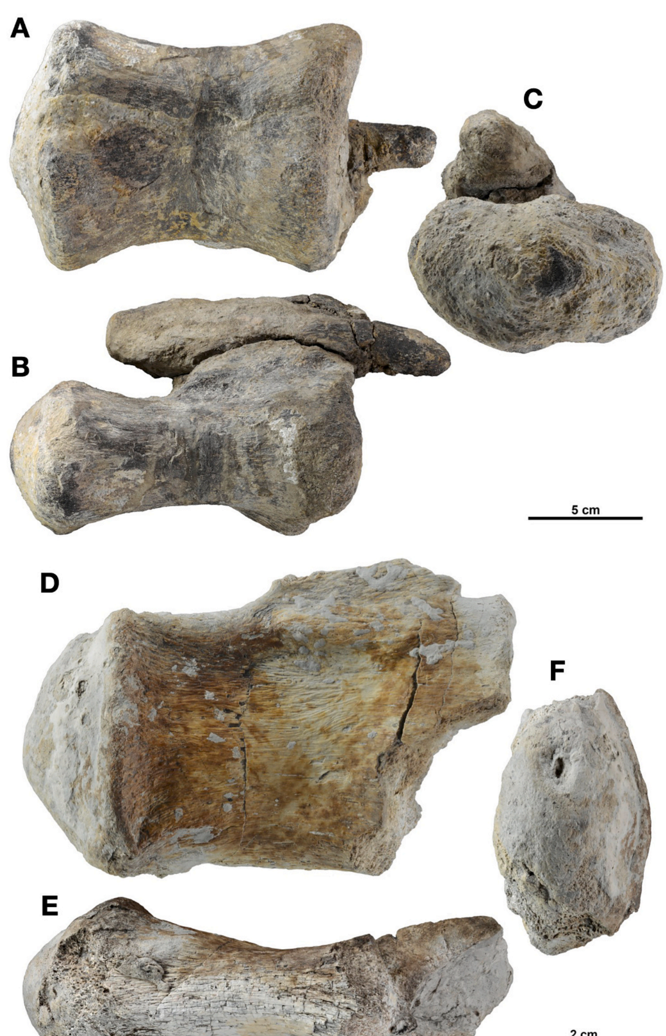

Fig. 13. A-C: Isolated caudal vertebra of *Titanosauria* indet (MPZ 2022/571) from CrG-1 site (late Campanian). A: Ventral view. B: Lateral view: C: Posterior view. **D-F:** Isolated caudal vertebra of *Titanosauria* indet (MPZ 2022/577) from CH-2 site (late Campanian). A: Lateral view. B: Ventral view. C: Posterior view.

The Cañalatorre site has provided nine vertebral centers. Six of them (MPZ 2022/572, 2022/574 to 2022/576, 2022/578 y 2022/579: Fig. 13D-F) have a similar size and morphology to that of MPZ 2002/571 described above. However, the most posterior vertebra (MPZ 2022/576) shows an amphicoelic centrum, a primitive condition of a character described in several South American titanosaurs (Salgado and Calvo, 1993). The other three vertebral centers (MPZ 2022/573, 2022/577 and 2022/580) of the Cañalatorre site present some differences, in particular a condylar groove in the posterior articular surface. A ventral depression, at least in the most anterior vertebral center (MPZ 2022/577) is present as in *Liranosaurus* (Sanz et al., 1999). These centers are more flattened lateromedially. However this difference is difficult to confirm due to the strong deformation of the bone specimens.

The presence of two medium-sized titanosaur sauropods of the Allueva Fm is consistent with current knowledge of these dinosaur faunas from southern Europe during the late Campanian (Sanz et al., 1999; Díez Díaz et al., 2016; Vila et al., 2022). In addition, some of the recovered caudal vertebrae show great similarity with *Lirainosaurus* from the late Campanian of the northern Castillian domain (Corral et al., 2016), which fits well the age of the upper Allueva Fm stablished in this work.

On the other hand, some few eggshell fragments have been recovered from the washing and sieving of the sediment samples picked up in Camino Negro and Cañalatorre sites. Three different ootypes have been recognized until now. The most significant type corresponds to prismatoolithid eggshells with prismatic structure and which display a striking dispersituberculate ornamentation, with their outer surface covered by nodes or tubercles. The nodes sometimes show pore openings on their tops, resembling crater-like structures. These features fit a priori with the oogenus *Pseudogeckoolithus* (Vianey-Liaud and López-Martínez, 1997), described from the Upper Cretaceous continental deposits of the Tremp Fm, in the South-Pyrenean basin. However, the sample is still very small to do proper and definitive ootaxonomical inferences, and thus we prefer to be cautious with their final assignation, classifying the Allueva Fm eggshells as cf. *Pseudogeckoolithus* sp. The other two types of eggshells recovered correspond to another theropod prismatoolithid eggshells but without ornamentation, and crocodylomorph eggshells with crocodyloid structure.

9. Review of the uppermost cretaceous dinosaur-bearing successions of northeast Iberia

During the Late Cretaceous, sedimentation in eastern Iberia took place in four major basins: the South-Pyrennean and the Basque-Cantabrian basins in the northern margin, the Iberian basin in the central interior areas, and the Betic basin in the southern margin. Between these basins, the South-Pyrenean basin has yielded one of the most rich and diverse record of Upper Cretaceous (uppermost Campanian-Maastrichtian) vertebrate fossils of Europe, with numerous fossil remains of dinosaurs, including hadrosauroid and rhabdodontid ornithopods, nodosaurid ankylosaurians, titanosaurian sauropods, and avian and non-avian theropods, along with other tetrapods such as crocodylomorphs, testudines, pterosaurs, squamates, and amphibians. This rich vertebrate fossil record is included in the coastal to continental successions of the Arén and Tremp formations (e.g. Llompart et al., 1984; López-Martínez et al., 2001; Canudo et al., 2016; Fondevilla et al., 2019; Pérez-Pueyo et al., 2021, and references therein). The Arén and Tremp formations includes also lower Maastrichtian sites with titanosaur eggs. The Tremp Fm preserves a rich terrestrial Maastrichtian track composed of multiple footprint localities with trackways made by titanosaurian sauropods, hadrosaurian ornithopods, as well as theropods (e.g. Riera et al., 2009; Vila et al., 2008, 2013). The fossil record of plant remains from the Tremp Fm sensu *lato* in Àger, Tremp and Vallcebre basins is also rich and includes both charophytes (e.g. Feist and Colombo, 1983; Villalba-Breva and Martín-Closas, 2013; Vicente et al., 2015, 2016) and vascular plants (e.g. Villalba-Breva et al., 2012; Marmi et al., 2015). Of particular interest for the present study in terms of comparison of the charophyte floras, it was the definition of a Maastrichtian charophyte biostratigraphy, well-correlated with magnetostratigraphic data, in the Àger and Vallcebre basins (Galbrun et al., 1993; Vicente et al., 2015, 2016, 2019).

Out of the South-Pyrenean basin, of particular relevance for the comparative analysis with the new dinosaur findings in the Allueva Fm is the presence of nearly time-equivalent fossil sites (i.e. mid-late Campanian to earliest Maastrichtian timespan) with abundant titanosaur sauropods across all the sedimentary domains of the Iberian basin. The map proposed for the palaeogeography Iberia around the end of the Campanian (Fig. 14) is an integration of the data obtained here with previously published information (in particular, Floquet, 1991; Alonso et al., 1993; García et al., 2004; Gil et al., 2010; Gómez-Gras et al., 2016; Vacherat et al., 2017; Martín-Chivelet et al., 2019a). The review of the dinosaur-bearing successions of the Iberian basin exposed below have been divided in six sedimentary domains (Fig. 15).

9.1. Northern Castillian domain

The northernmost part of the Iberian basin reviewed here is represented by the northern part of the Castillian domain. There, a

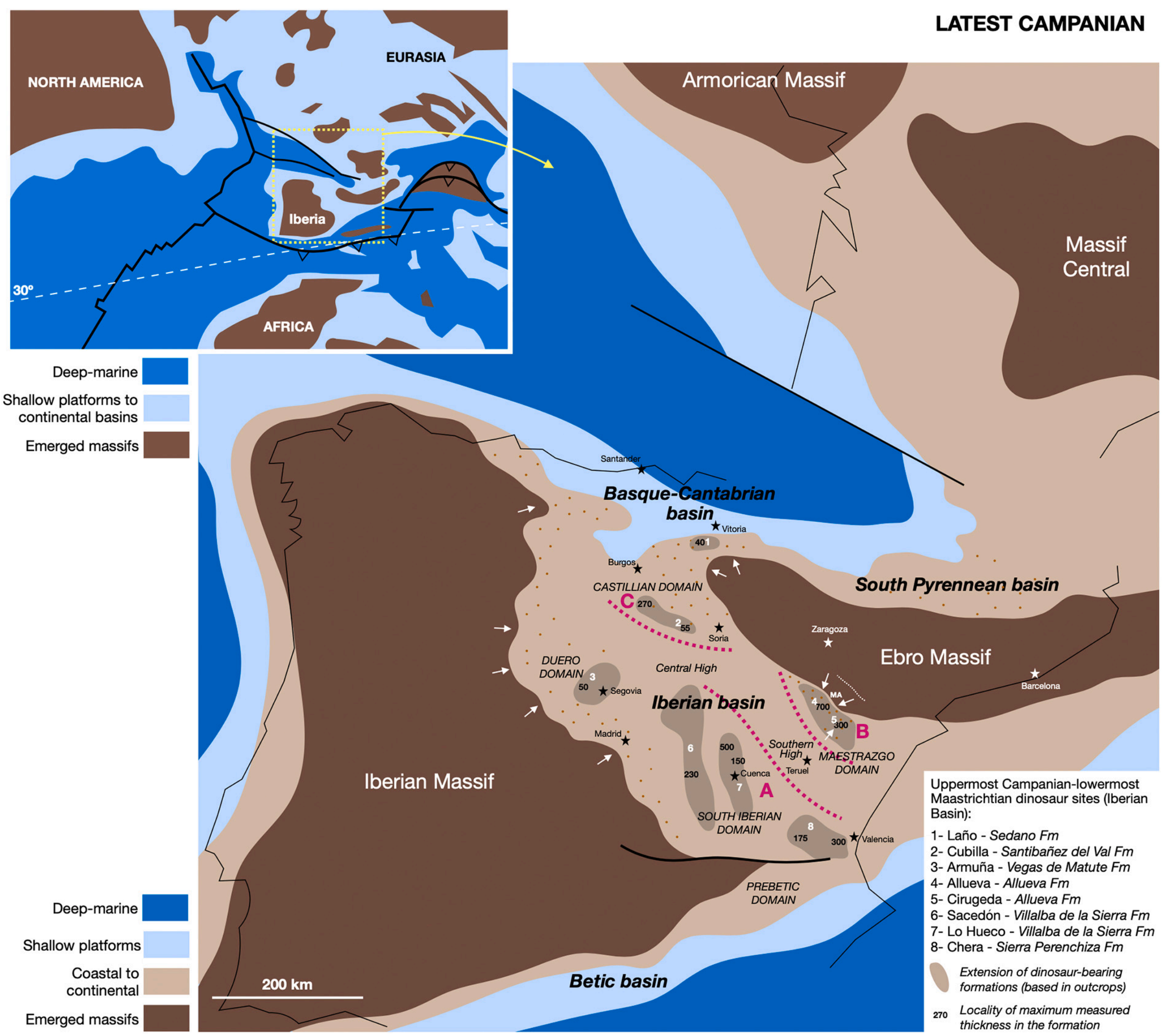

Fig. 14. Palaeogeography of Iberia at the end of the Campanian indicating the extension of the formations including upper Campanian–lowermost Maastrichtian fossil sites with titanosaur sauropods. Data mostly compiled from Floquet (1991), Alonso et al. (1993), García et al. (2004), Gil et al. (2010), Gómez-Gras et al. (2016), Vacherat et al. (2017), and Martín-Chivelet et al. (2019a). The inset in the upper left have been modified from Barrier et al. (2018). Notice that the dinosaur-bearing formations cover different chronostratigraphic intervals (see Fig. 15). White arrows indicates the source areas for terrigenous input. The white dashed line in the Ebro massif shows the northern extension of the post-rift Cenomanian-Santonian outcrops (see Aragües et al., 1981) previous to the uplift of the Montalbán anticline (MA). Three zones A-B-C (in purple) had different subsidence evolution in the Iberian basin (see text for explanation). (For interpretation of the references to colour in this figure legend, the reader is referred to the web version of this article.)

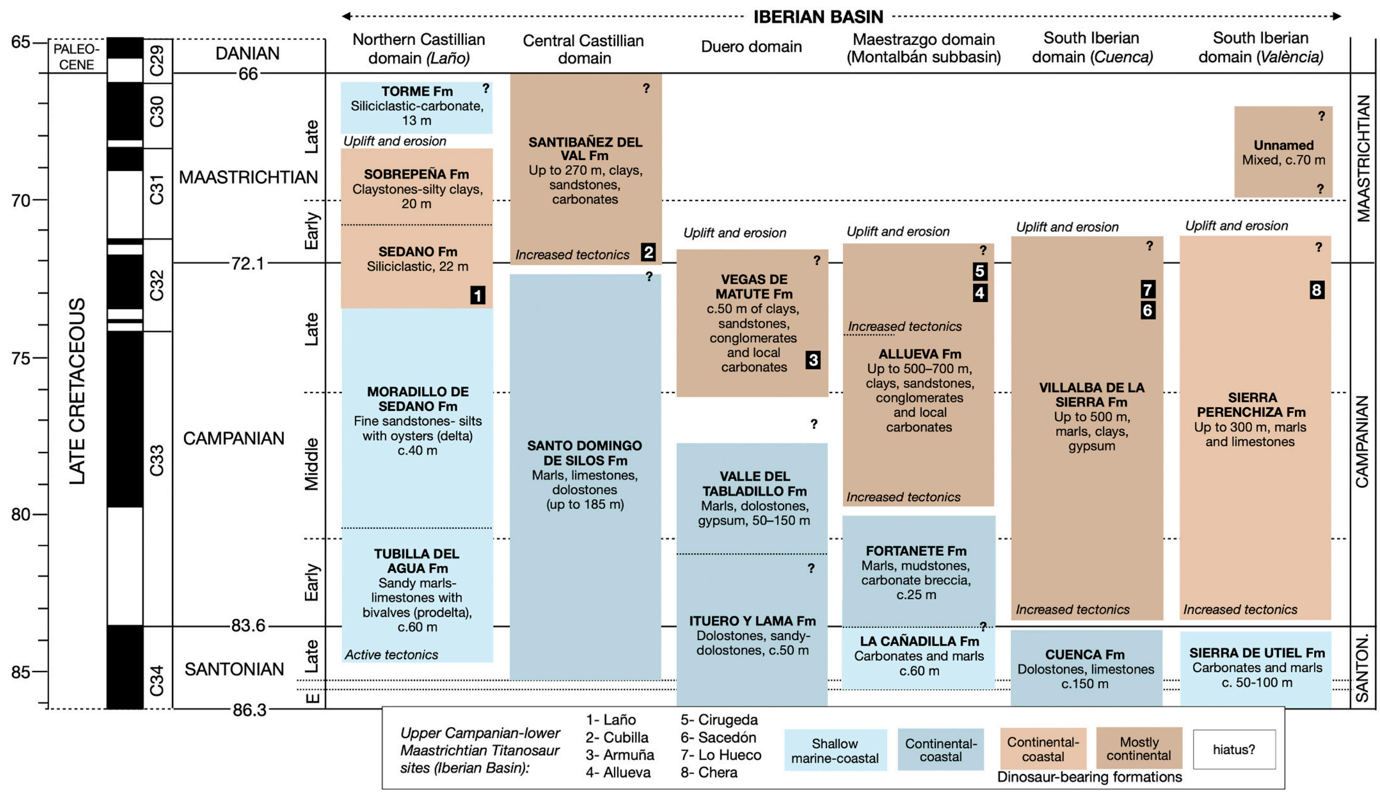

Fig. 15. Summary of the Campanian–Maastrichitian stratigraphy of different domains of the Iberian basin (see Fig. 14 for location of fossil sites). Data in the Castillian, Duero and South Iberian domains mostly complied from Floquet (1991), García et al. (2004), Gil et al. (2010), Corral et al. (2016), and Martín-Chivelet et al. (2019a). Time scale from Haq (2014).

Campanian transgressive event sourced from the north involved the widespread setting of a shallow marine platform, and most of the domain was covered by the carbonates with abundant rudists represented by the Quintanaloma Fm (Floquet, 1991; Martín-Chivelet et al., 2019a). The lateral extent of this shallow-marine platform was progressively reduced (to the north) due to a middle-late Campanian forced regression, which has been related to tectonic uplift (e.g. Martín-Chivelet et al., 2019a). To the east (Laño area) the uppermost Santonian-Campanian succession is marked by the progradation of the deltaic system of the Tubilla del Agua and Moradillo de Sedano formations. This deltaic system is overlain by the subtidal to supratidal oyster bearing terrigenous-dominated unit Sedano Fm (Floquet et al., 1982). The latest Campanian-earliest Maastrichtian Sedano Fm (Corral et al., 2016) unit grades to the east to fluvial-deltaic siliciclastics, that include the Laño fossil site.

The Laño site is latest Campanian in age (i.e. lower part of the subchron C32n; Corral et al., 2016). This site (see 1 in Fig. 15) has yielded a very diverse continental vertebrate assemblage, with remains of bony fishes, amphibians, lizards, snakes, turtles, crocodrylomorphs, pterosaurs, dinosaurs and mammals (Astibia et al., 1999; Pereda-Suberbiola et al., 2000, 2015; Isasmendi et al., 2022). It includes also very abundant remains of titanosaurian sauropods, that have been assigned to the taxon *Liranosaurus astibidae* defined in this locality (Sanz et al., 1999; Díez-Díaz et al., 2011, 2013). In Laño, the Sedano Fm is overlain by the clayed Sobrepeña Fm. This unit was deposited around the early-late Maastrichtian transition in coastal plains, and includes dinosaur, crocodylomorph and turtle remains in the Urria area (Floquet, 1991; Berreteaga, 2008; Berreteaga et al., 2008). The upper Maastrichtian calcareous sandstones and limestones of the Torme Fm unconformably overlies the Sobrepeña Fm. A low-angle erosive unconformity found between these two units resulted from a combination of uplift and tilting of the sedimentary area, coupled with a regional sea transgression (i.e. intra-Maastrichtian unconformity in Baceta et al., 1999). The Tormé Fm includes interbedded terrigenous levels rich in vertebrate fauna, such as the Albaina fossil site (Berreteaga, 2008). An erosive surface followed by a major transgressive event marks the setting of the Paleocene carbonate platform (Baceta et al., 1999).

9.2. *Central Castillian domain*

In the central part of the Castillian domain, marine incursions sourced from the north left the local record of shallow marine levels in the continental-coastal carbonates of the Santo Domingo de Silos Fm (Floquet, 1991). This unit consist of an up to 185 m-thick succession of dolostones, marls, and micritic limestones, and has been regarded as deposited either during the late Santonian–Campanian (Floquet et al., 1982; Alonso et al., 1993; Martín-Chivelet et al., 2019a), or during the early–middle Campanian (García et al., 2004). After a major discontinuity on top of the Santo Domingo de Silos Fm, the continental succession of the Santibañez del Val Fm is dominated by red clays and cross-bedded sandstones alternating with lacustrine-palustrine micritic limestones with gastropods, charophytes, ostracods and oncoids.

The Santibañez del Val Fm includes in its lower part an up to 270 m-thick uppermost Cretaceous succession. The early Maastrichtian age assigned to the lower levels of the Santibañez del Val Fm is based on the identified malacofauna and charophyte assemblages (Floquet, 1991; Floquet et al., 1994; Feist and Floquet, 2022). Dinosaur eggshells and bone remains are locally present, with different fossil sites in the Soria and Burgos provinces. Of particular interest are the findings of Lapparent et al. (1957) in the locality of Cubilla in the basal levels of the c.50 m-thick Santibañez del Val Fm (see 2 in Fig. 15). Main findings are a tibia attributed to a *Rhabdodon*, and a posterior caudal vertebra, that was assigned to a basal titanosuarian in Pereda-Suberbiola and Ruiz-Omeñaca (2001). Dinosaur eggshells have been also studied in this formation west to Cubilla, in the nearby La Tejera site (Moreno-Azanza et al., 2016).

9.3. Duero domain

In the westernmost marginal areas of the Iberian basin represented by the Duero domain sedimentation was irregular, with frequent stratigraphic gaps (Gil et al., 2010). There, the Santonian–lower Campanian represents a sedimentary sequence bounded by major unconformities. This succession is formed by a coastal succession with the dolostones and sandy-dolostones of the Ituero y Lama Fm, and the continental marls (with local gypsum), dolostones, and collapse-breccias of the Valle del Tabladillo Fm. This unit is bounded on top by a karstic surface, associated to a stratigraphic gap of uncertain extent (García et al., 2004; Gil et al., 2010). The karst is overlain by the c.50 m thick-continental siliciclastic succession of the Vegas de Matute Fm. The precise age of this formation is uncertain, and was tentatively assigned to the late Campanian (Gil et al., 2004, 2010), or to the late Campanian–earliest Maastrichtian (Pérez-García et al., 2016). The unit is bounded on top by a major unconformity associated to a Maastrichtian–lower Eocene stratigraphic gap (Armenteros et al., 2002).

The Vegas de Matute Fm includes sandstones levels with the fossil sites of Carbonero el Mayor and Armuña in its lower part (Buscalioni and Martínez-Salanova, 1990; Pérez-García et al., 2016; see 3 in Fig. 15). A number of taxa has been recognized in these sites, with actinopterygid fishes, turtles, lepidosaurs, crocodylomorphs, an indeterminate member of lithostrotian titanosaur, a theropod attributed to cf. *Arcovenator*, and an ornithopod identified as cf. *Rhabdodon*. In the area located around these fossil sites, the unit was deposited in a fluvial system with local marine influence (Pérez-García et al., 2016). In more western marginal areas, the unit represents a prograding braided system changing from humid to semiarid climate (Fernández-Garcia et al., 1989).

9.4. Maestrazgo domain

The Santonian–Campanian succession of the northern part of the Maestrazgo domain includes the La Cañadilla, Fortanete and Allueva formations (Fig. 15). The La Cañadilla Fm has a relatively homogenous thickness and sequential distribution across the Maestrazgo domain, and has been regarded as deposited during a stage of relative tectonic quiescence, with the possible inprint of the sea level changes formed in tune with the eccentricity orbital cycle (Torromé et al., 2022). In contrast, the overlaying Fortanete Fm records thickness (20–90 m) and lithological changes (carbonate breccias, marls, micritic limestones, gypsum) across the Maestrazgo domain that indicates a more heterogenous distribution of the subsidence. The data reported here indicates that the Fortanete Fm was mostly deposited during the early Campanian, in the subchron C33r.

The Fortante Fm is abruptly overlain by the Allueva Fm. The thickness of this unit is variable across the Montalbán and Aliaga subasins ranging from 300 to 700 m (see Table 1). In the Montalbán subbasin, the upper part of the unit includes an uppermost Campanian vertebrate fossil association of the Allueva sites (see 4 in Fig. 15), with the common presence of titanosaurs described above. In the nearby Aliaga subbasin, the fossil site of Cirugeda located in the upper part of the Allueva Fm (see 5 in Fig. 15) includes a fragment of a neural spine of *Titanosauria* indet., and remains of testudines attributed to cf. *Solemys* sp. (Canudo et al., 2005). The onset of the sedimentation of the Allueva Fm marks the initial phases of uplift of the Montalbán anticline with the coeval formation of the highly subsident continental Montalbán subbasin. Sedimentation was interrupted around the onset of the Maastrichtian, and resumed probably during the middle Eocene (Pérez et al., 1983; Casas et al., 2000).

9.5. South Iberian domain (Cuenca)

In the northern part of the South Iberian domain (Cuenca province), the Campanian-Maastrichtian sedimentation occurred mostly in continental settings. There, the c. 150 m-thick peritidal-sabkha massive carbonate breccias of the Cuenca Fm were assigned to the Coniancian–Santonian stages (Martín-Chivelet et al., 2019a). This unit is overlain by a major sedimentary discontinuity related to a tectonic event (Martín-Chivelet et al., 2019a), with the abrupt setting of the mixed carbonate-evaporite depositional system of the Villalba de la Sierra Fm. This formation consists of marls, clays and gypsum deposited in lacustrine-palustrine environments, and muddy floodplains with distributary sandy channels. The thickness of the unit in its type locality is 157 m, but it may locally reach up to 500 m (Vilas et al., 1982). The Villalba de la Sierra Fm contains a rich assemblage of charophytes (Grambast, 1975; Grambast and Gutiérrez, 1977), and has been regarded as deposited during the Campanian-earliest Maastrichtian (Martín-Chivelet et al., 2019a).

The upper part of the Villalba de la Sierra Fm embraces the fossil site of Lo Hueco (see 7 in Fig. 15), which has yielded a rich collection of well-preserved vertebrates, including actinopterygians and teleosteans fishes, amphibians, panpleurodiran (bothremydids) and pancryptodiran turtles, squamate lizards, eusuchian crocodylimorphs, rhabdodontid ornithopods, theropods (mainly dromaeosaurids), and titanosaur sauropods (Ortega et al., 2015). Westwards, near the locality of Sacedón (northern Sierra de Altomira; see 6 in Fig. 15), the upper part of the Villalba de la Sierra Fm includes a caudal vertebra of a titanosaur sauropod (Ortega and Pérez-García, 2009), as well as a rich assemblage of dinosaur eggs (Sanguino et al., 2021).

9.6. South Iberian domain (València)

In the southern part of the South Iberian domain (València province), the Sierra the Utiel Fm represents cyclic sedimentation in a very shallow-marine to peritidal carbonate platform, with a wide spectrum of facies ranging from miliods and rudist-rich limestones to black-pebble breccias (e.g. Vilas et al., 1982; Martín-Chivelet and Giménez, 1992). The unit was regarded as deposited during the late Santonian-earliest Campanian (Alonso et al., 1991; García et al., 2004), during the latest Coniacian-earliest Santonian (Martín-Chivelet and Giménez, 1992), or during the Coniancian–Santonian, coeval to the Cuenca Fm (Martín-Chivelet et al., 2019a). Moreover, the possible lateral equivalence between the Sierra de Utiel and La Cañadilla formations (Fig. 15) is supported by the similar sequential arquitecture of the units (probably related to allocyclic control), and by the common presence of marine rudist-rich levels sourced from the southern open marine areas (Martín-Chivelet and Giménez, 1992; Torromé et al., 2022). The Sierra de Utiel Fm is bounded on top by a major regional unconformity, which has been linked to a tectonic event (Martín-Chivelet et al., 2002, 2019a).

Overlying the unconformity on top of the Sierra de Utiel Fm, the Campanian–earliest Maastrichtian Sierra Perenchiza Fm consist of marls and limestones with abundant charophytes, ostracods and gastropods deposited in lacustrine-palustrine environments, with the episodic setting of coastal lakes, wetlands and salty marshes (Vilas et al., 1982; Alonso et al., 1991). The unit is very variable in thickness, ranging from 15 to 300 m. In the Chera-Buñol area (see 8 in Fig. 15), the Sierra Perenchiza Fm is up to 50 m-thick and includes vertebrate fossil sites with dinosaurs, crocodylimorphs and turtles (Company, 2004; Company et al., 2009). Of particular interest are titanosaurian remains, some of them assigned to *Lirainosaurus* (Díez-Díaz et al., 2015). A palynological study of the Chera site indicates the presence of wetlands with ephemeral to semi-permanent ponds and lakes (Peyrot et al., 2020). Palynological and palaeomagnetic data (Pueyo et al., 2014) suggest a late Campanian-early Maastrichtian age for the Chera fossil site.

In the València province, the Sierra de Perenchiza Fm is locally unconformably overlain by an unnamed unit with mudstones and interbeded fluvial sandstones. This unit have similar stratigraphic position of the Cerrillares Fm (Martín-Chivelet, 1994; Martín-Chivelet et al., 2019a). It includes the La Solana site (Tous area), that has yielded a diversified continental fauna with remains of bony fishes, lissamphibians, chelonian remains (*Solemys* sp.), crocodylomorphs and pterosaurs. Dinosaurs are also abundant, with a basal hadrosaurid and scanty titanousaurian material (e.g. Company et al., 2009). The occurrence of a rich charopyte flora (Company, 2004) along with palaeomagnetic data (Pueyo et al., 2014) indicates a late Maastrichtian age for La Solana site.

10. Discussion

10.1. Equivalence between Allueva Fm and tecto-sedimentary units: Implications

As demonstrated here, large subsidence rates of the Montalbán subbasin during the latest Cretaceous (mostly during the middle and late Campanian) involved the sedimentation of the up to 500–700 m-thick Allueva Fm. The reported data brings some review to previous work assigning a Paleogene age to the lower continental units recorded in the different intramountain subbasins developed around the Montalbán anticline.

In a regional stratigraphic synthesis, Pardo et al. (1989) defined successive tecto-sedimentary units (TSUs) in the subbasins found north and south to the Montalbán anticline, and in the south-central Ebro basin. The methodology of the tecto-sedimentary analysis (Garrido-Megías, 1973) implemented in Pardo et al. (1989) is based in the identification of genetic stratigraphic units termed tecto-sedimentary units (TSUs). These consist of sedimentary successions with a definite vertical trend (either fining or coarsening upward) bounded by regional unconformities and their correlative conformities. In the tecto-sedimentary analysis, coarsening and fining upward evolutions are related to basinwide stages of increasing and decreasing tectonic activity respectively, and it is assumed that each TSU characterized in a basin has chronostratigraphic significance (e.g. Pardo et al., 1989; Pérez-Rivares et al., 2018). Following this methodology, the analysis of the syntectonic successions recorded in the foreland Ebro basin resulted in the identification of eight tecto-sedimentary units (TSUs T1 to T8), which were dated as late Paleocene–middle Miocene (e.g. Villena et al., 1996; Muñoz et al., 2002; Pardo et al., 2004).

The alpine compression involved the formation of a set of isolated intramountain subbasins in the interior areas of the Iberian Ranges. Four of these subbasins developed around the Montalbán anticline, the Aliaga and Montalbán subbasins to the south, and the Berge and Alloza subbasins to the north (Fig. 2A). As explained above, the sedimentary record of the Montalbán subbasin was divided in TSUs M1–M5 (Pérez et al., 1983; Casas et al., 2000). Pardo et al. (1989) proposed a late Paleocene-Eocene age for TSUs M1 and M2 based in regional correlation (Fig. 16A). However, the age calibration of the Allueva Fm reported here indicates a middle-late Campanian age for the TSU-M1, and a latest Campanian earliest Maastrichtian age for the lower part of TSU-M2 (Fig. 16B). Moreover, the nearby Aliaga subbasin was divided in TSUs A1–A6 (González, 1989), which were regarded as age equivalent to the TSUs identified in the Montalbán subbasin. The upper levels of the TSU-A1 include the dinosaur fossils of the Cirugeda site (Canudo et al., 2005). In the Aliaga subbasin, the boundary between the TSUs-A1 and A2 is an erosive angular unconformity (González and Guimer, 1993). This unconformity is here regarded as possible lateral equivalent to the unconformity identified between the Allueva Fm and the *Paleogene unit* in the Montalbán subbasin (Fig. 16B).

Northwards to the Montalbán anticline, the age of the oldest continental unit recorded in the Berge and Alloza subbasins (i.e. TSU-T1 in Pardo et al., 1989) was dated as late Paleocene middle Eocene (Fig. 16A). This age assignment was indicated by the presence of the Eocene continental gastropod *Vidaliella gerundensis* Vidal, 1983, and by regional correlation with equivalent units of the South Ebro Basin (Pardo et al., 1989). Moreover, there is a widespread regional angular unconformity between the underlaying marine Cretaceous carbonate units and the TSU-T1, which is associated to a large erosive gap of variable amplitude (e.g. González, 1989). The data presented in our work indicates that this TSU-T1 is not coeval to the TSUs A1 and M1 defined in the Aliaga and Montalbán subbasins respectivelly.

In summary, the results presented here indicate that the latest Cretaceous-Paleogene tectonic evolution left a particular record of genetic TSUs in the intramountain subbasins developed north and south to the Montalbán anticline respectively. This shows that much caution should be paid in the use of the tecto-sedimentary analysis as a tool to

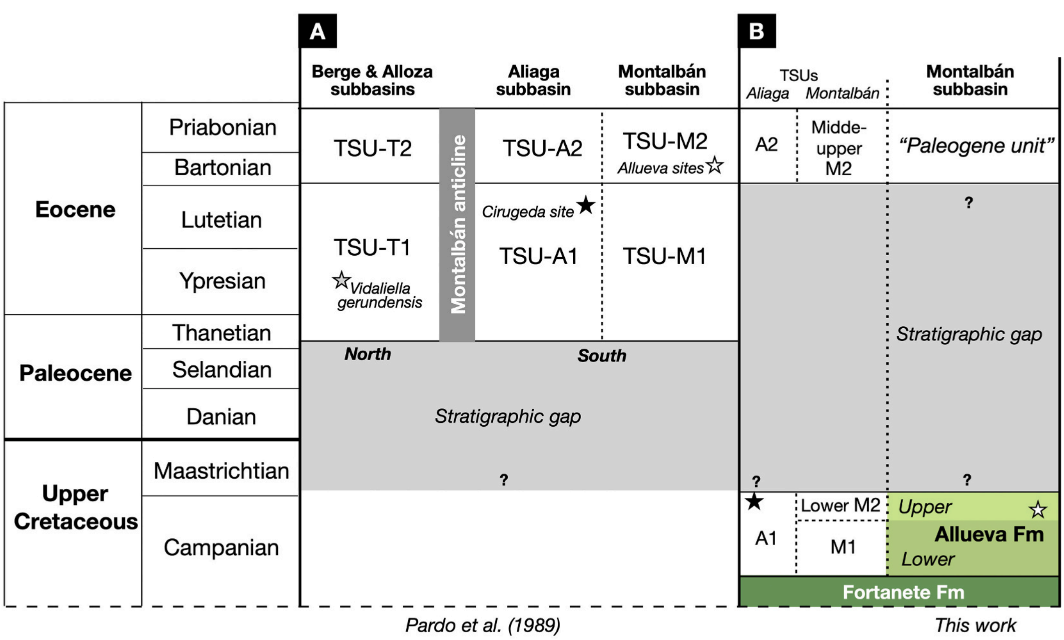

Fig. 16. A: Stratigraphy of the older tecto-sedimentary units (TSUs) recorded in the subbasins located north and south to the Montalbán anticline (according to Pardo et al., 1989). **B:** Equivalence between the TSUs A1-A2/M1-M2 and the Allueva Fm defined in this work.

correlate the sedimentary successions found in separated intramountain subbasins. At local scale, the movement of individual structures control the formation of local unconformities and the imprint of particular facies trends in the syntectonic sedimentary successions (e.g. Santanach, 1989; Santolaria et al., 2015), but this observation cannot be assumed to occur at larger regional scale.

10.2. Implications for the latest Cretaceous palaeogeographic evolution of the Iberian basin

The compressional regime in the central and eastern Iberian Ranges occurred mostly during the Eocene-early Miocene (e.g. Casas et al., 2000; Capote et al., 2002; Antolín-Tomás et al., 2007). However, the presence of the middle-late Campanian continental Allueva Fm indicates that the initial phases of uplift of some large-scale structures of the northeastern Iberian Ranges, such as the Montalbán anticline started earlier, during the latest Cretaceous. Southwards to this incipiently uplifted area, the northern margin of the Montalbán continental subbasin studied here accommodated the 500–700 m-thick Allueva Fm.

The latest Cretaceous synsedimentary tectonics in the Iberian basin have been recently reviewed in Martín-Chivelet et al. (2019a). These authors point out that although the stress intensity and tectonic activity has notable spatial variability across the different domains, the timing of tectonic pulses in the various subbasins and domains of the Iberian basin was nearly isochronous. They differentiate two major latest Cretaceous tecto-sedimentary stages: (1) a latest Santonian initiation of convergence, with drastic palaeogeographic reorganization and new subsidence patterns in the Basque-Cantabrian basin, in the northern Castillian platform and in the Southern Iberian domain; and (2) a late early Maastrichtian-late Maastrichtian stage of renovated contractive tectonism affecting not only the Pyrenees and the Basque-Cantabrian basin, but also different domains of the Iberian basin. Moreover, the data reported here shows further stages of tectonic reactivation during the middle part of the middle Campanian (with the initial uplift of the Montalbán anticline), and during the middle part of the late Campanian (with sharp increase of the subsidence rates in the Allueva Fm).

The Aliaga and Montalbán subbasins appear at present as two well-differentiated intramountain basins separated by the Utrillas thrust (Fig. 2A). However, the formation of this large thrust structure occurred after the sedimentation of the Allueva Fm, onwards from the Eocene-Oligocene transition (González and Guimer, 1993; Simón and Liesa, 2011). Therefore, most probably there was a connection between the Aliaga and Montalbán subbasins during the sedimentation of the Allueva Fm. The local presence of conglomeratic beds dominated by calcareous pebbles (mostly sourced from Jurassic and Upper Cretaceous marine carbonate rocks) in different intervals of the Allueva Fm indicates the presence of a proximal source area involving the uplift and erosion of Mesozoic rocks. The dominant palaeocurrent data measured in the northern margin of the Montalbán subbasin shows that the source area was the incipiently uplifted Montalbán anticline (see also Pérez et al., 1983). However, in the Aliaga subbasin palaeocurrent and overall facies distribution indicates that this detrital calcareous material was also supplied from the southern marginal areas (González and Guimer, 1993; Gónzalez and Pérez, 2018). Following the interpretation of previous work (i.e. González and Guimer, 1993), in the late Campanian palaeogeography reconstructed here it is suggested the presence of a broad uplifted area located south to the Aliaga and Montalbán subbasins, which is named Southern high (Fig. 14).

It is interesting to note that north to the Montalbán anticline, around to the Sierra de Arcos thrust (see Fig. 2A for location) occur the northernmost Upper Cretaceous outcrops of the northeastern Iberian Ranges. There, a 35 m-thick peritidal to shallow marine carbonate succession includes biostratigraphic markers (benthic foraminifera, rudists) that suggest an irregular and condensed sedimentation during the Cenomanian–Santonian in this marginal marine area (Ríos-Aragües et al., 1981). The uplift of the area located north to the Montalbán subbasin during the Campanian resulted in the exposure of this peritidal-shallow marine area (see white dashed line in Fig. 14). In coherence to most of the available paleogeographic reconstructions of north Iberia (e.g. Martín-Chivelet et al., 2019a), this elevated area could be regarded as a southern expansion of the Ebro massif. The presence of the elevated area of terrigenous supply of the Ebro massif is evidenced not only during the latest Cretaceous, but in other Mesozoic intervals. For instance, the existence of the Ebro massif during the Late Jurassic is indicated by the distribution of siliciclastic-rich intervals in the Oxfordian–Kimmeridgian units of the northern Soria Seaway (e.g. Aurell et al., 2003), or during the Early Cretaceous, with the northern terrigenous clastic input in the Barremian–Aptian of the Oliete subbasin (e.g. Liesa et al. in Martín-Chivelet et al., 2019b; García-Penas et al., 2022).

Onwards from the earliest Maastrichtian, the sedimentary area in the Iberian basin became mostly restricted to the Castillian domain (Fig. 15). In the central and southern Iberian basin there are few evidences of development of subsiding areas during the Maastrichtian, and has been also suggested an uplift and erosion of the Duero domain (e.g. Gil et al., 2010; Pérez-García et al., 2016), of the northern Maestrazgo domain (this work), and of the South Iberian domain, where only the continental Cerrillares Fm is locally recorded (Martín-Chivelet et al., 2019a). In contrast, in the central areas of the Castillian domain there are two continental subbasins (i.e. the Arganza-Talveila-Cubillos and the Covarrubias-Santo Domingo de Silos subbasins) separated by a threshold, that according to Floquet (1991) originated from a local tectonic uplift. It is also suggested that the widespread regressive event observed in the northern Iberian basin at the latest Cretaceous could also be favoured by the general long-term Maastrichtian sea level fall (e.g. Haq, 2014).

In summary, the reported review shows evidences of successive stages of tectonic activity during the latest Cretaceous initial stages of Africa-Europe-Iberia convergence (e.g. Dercourt et al., 1986; Visser and Meijer, 2012; Dielforder et al., 2019), which have variable intensity over space and time. This resulted in significant differences in the stratigraphy (age, thickness, and lithology) of the continental-dominated formations coevally deposited in the interior areas of the Iberian basin. According to the age proposed by different authors for the boundaries of the latest Cretaceacous units of the Iberian basin (some of them still open to discussion: see questions marks in Fig. 15), three stages of palaeographic evolution are proposed:

- Around the Santonian-Campanian transition, the onset of the sedimentation of the thick-continental carbonate-evaporite dominated successions (with scarce terrigenous input) of the Villalba de la Sierra and Sierra Perenchiza formations indicates a major palaeogeographic rearrangement of the South Iberian domain (see zone A in purple, Fig. 14). Local development of highly subsident subbasins (thickness up to 500 m during the entire Campanian) occurred in relatively interior areas of the basin. Westwards, the relatively low subsiding area located close to the Iberian massif in the Duero domain had significant terrigenous influence (i.e. Vegas de Matute Fm; Gil et al., 2010). Eastwards, in the Maestrazgo domain, sedimentation rates and terrigenous input during the sedimentation of the lower Campanian Fortanete Fm was relatively low, with no evidences of tectonic uplift of the northern marginal areas.
- During the middle-late Campanian, the Aliaga and Montalbán subbasins developed in the northern Maestrazgo domain (see zone B in purple, Fig. 14). Large subsidence rates allow the accumulation of the 300–700 m-thick terrigenous-dominated successions of the Allueva Fm, with a further stage of increase of tectonic activity during mid-late Campanian to explain the sharp increase in subsidence rates. Northwards, the southern flank of the Montalbán anticline (probably representing the southern margin of the Ebro massif) was uplifted. Certain areas of the Southern high were also probably uplifted, and supplied detrital material to the Aliaga subbasin.

Further south, continental sedimentation in the subsident areas of the South Iberian domain persisted (see zone A in purple, Fig. 14).

- Onwards from the earliest Maastrichtian sedimentation in most of the South Iberian, Maestrazgo and Duero domains was scarse. Northwards, local subsiding subbasins developed in the central part of the Castillian domain, with the sedimentation of the mixed-succession of the up to 270 m-thick Santibañez del Val Fm (see zone C in purple, Fig. 14). Moreover, in the northern Castillian domain, there are evidences of tectonic activity during the mid-late Maastrichtian, as indicated by the angular unconformity between the Sobrepeña and Torme formations (i.e. intra-Maastrichtian unconformity, Baceta et al., 1999).

During the three stages of palaeogeographic evolution summarized above, the areas of the Iberian basin represented by the Central and Southern highs (Fig. 14) remained probably uplifted. Marine incursions sourced from the north reached the Castillian domain during most of the Campanian (e.g. Floquet, 1991), whereas those sourced from the south left peritidal-shallow marine intervals only in the late Santonian-earliest Campanian successions recorded in the South Iberian and Maestrazgo domains (e.g. García et al., 2004; Torromé et al., 2022).

The newly defined Allueva Fm is also relevant in terms of vertebrate paleontology, specially related to dinosaurs. It is nowadays widely accepted that across the late Campanian-early Maastrichtian, a faunal turnover took place in the Ibero-Armorican landmass (Csiki-Sava et al., 2015), which affected primarily to herbivorous dinosaurs. This change of faunas was firstly reported by Le Loeuff et al. (1994) and supported and characterized lately by other authors (López-Martínez et al., 2001; Pereda-Suberbiola et al., 2003; Csiki-Sava et al., 2015; Sellés and Vila, 2015; Vila et al., 2016). Apparently, the preturnover communities were dominated by titanosaurian sauropods, rhabdodontids ornithopods and struthiosaurine ankylosaurs, which were all replaced by hadrosauroid ornithopods and different titanosaurian, probably coming from Asia the first and from Gondwana the second. The turnover happened in the early part of the late Maastrichtian, around the C31r-C31n reversal (Fondevilla et al., 2019), and though both pre and post turnover faunas coexisted for around 1.2 Ma, soon the hadrosauroids became the predominant herbivorous fauna. By this reason, the Allueva Fm (middle-late Campanian in age) becomes an interesting geological unit to characterize and add information to the knowledge of the dinosaur assemblages that inhabited Iberia prior to the faunal turnover. Any future finding would help to give new answers to this topic.

11. Conclusions

The uppermost Cretaceous Allueva Fm defined in this work is a continental terrigenous-dominated unit deposited in the early tages of formation of the Montalbán and Aliaga subbasins of the northeastern Iberian basin (Maestrazgo domain, Spain). Paleomagnetic data constrained with charophyte biostratigraphy indicates that the Allueva Fm was deposited during the middle-late Campanian subchron C33n, and during most of the latest Campanian-earliest Maastrichtian C32 chron. This new age calibration involves major revision of the stratigraphy proposed in previous regional stratigraphic work, which regarded this unit as deposited during the Paleogene.

The Allueva Fm is a red mudstone-dominated succession, including intercalation of cross-bedded to massive- bioturbated sandstones and conglomerates dominated by calcareous pebbles, with local presence of gypsum-rich levels and carbonates. The overall distribution of the distinguished facies associations indicates that the unit was deposited in the middle-distal areas of an alluvial system, with sandstone-conglomeratic distributary braided fluvial channels. Mudflats with common interstitial gypsum as a result of the reduced supply of water and terrigenous sediment are found in the middle part of the Allueva Fm. The abrupt setting in the upper part of the Allueva Fm of a large lacustrine-palustrine carbonate area with evidence of intense microbial activity (micritic mounds, oncolites) has been related to an increase of water input. Most of the dinosaur fossil sites in the Allueva Fm occur in the marginal areas of this lacustrine system.

A remarkable fossil assemblage of vertebrates found in the upper part of the Allueva Fm correspond to the latest Campanian (i.e. C32n cronozone), previous to the faunal turnover that took place in the Ibero-Armorican landmass in the early part of the late Maastrichtian. The vertebrate association of Allueva consist of abundant archosaurs with the widespread presence of titanosaur sauropod dinosaurs. Otherwise, of particular biostratigraphic interest is the charophyte-rich level found in the vertebrate fossil site of Cañalatorre, which includes *Bymochara conquensis, Strobilochara* cf. *diademata,* and *Peckichara cristatella* among other species. This assemblage was previosly assigned to the late Campanian-early Maastrichtian time range, but it is now constrained in the Montalbán subbasin to the latest Campanian.

The Allueva Fm includes successive conglomeratic levels with abundant poorly sorted calcareous pebbles, which were sourced from the erosion of previous Jurassic and Cretaceous marine rocks. Palaeocurrent data indicates the presence of a northern source area. This indicates the incipient uplift and erosion of the Montalbán anticline coeval to the sedimentation of the Allueva Fm at the middle-upper Campanian. An increase of sedimentary rates (from average rates of c.4 cm/Ky to 19 cm/ky) observed in the lower part of the Allueva Fm has been related to a stage of increasing tectonic activity around the boundary between magnetozones C33/C32 (i.e. midde part of the late Campanian).

The observations provided in this work after the comparative review of the contiental latest Cretaceous dinosaur-bearing successions recorded across the different sedimentary domains of the Iberian basin should have to be accounted in future reconstructions of the geodynamic evolution of northeast Iberia during the latest Cretaceous. Some of the observations listed below have to be regarded as preliminary, until a precise age calibration is reached for all the uppermost Cretaceous continental sedimentary successions of the Iberian basin. The success of the approach used in this work to calibrate the age of the Allueva Fm (combining charophyte biostratigraphy and magnetostratigraphy) opens the possibility to reach this objective. The review of the available data reported here indicates that:

- Sedimentation during the Campanian-Maastrichtian was irregularly distributed in the interior areas of the Iberian basin, with a patchy distribution of the subsiding continental-dominated areas. This contrasts with the relatively large lateral extension of the shallow marine carbonate ramps developed in wide areas of the Iberian basin during the previous Cenomanian–Santonian post-rift stage. Onwards from the Campanian, marine influence in the Iberian basin became mostly restricted to the northern Castillian domain.
- A number of locally highly subsident continental subbasins start to develop in the interior areas of the Iberian basin at different time intervals, with a south to north migration of the tectonic deformation: during the Campanian in the South Iberian domain, during the middle-late Campanian in the Maestrazgo domain, and mostly during the Maastrichtian in the central Castillian domain.
- In the southern and central areas of the Iberian basin, the larger subsidence and sedimentation rates occur locally during the middle-late Campanian with the development of the continental Montalbán subbasin in the Maestrazgo domain (up to 500–700 m-thick Allueva Fm), and during the whole Campanian in the South Iberian domain (up to 500-m thick Villalba de la Sierra Fm). In contrast, the Maastrichtian sedimentary record is poorly represented in the central and southern areas of the Iberian basin, resulting in the presence of a wide sedimentary gap that probably embraces also most of the Paleocene.
- In all the latest Cretaceous continental subbasins of the Iberian basin, dinosaur fossil sites including abundant titanosaurs and ornithopods

are concentrated in a relatively narrow timespan from late Campanian to earliest Maastrichtian.

Declaration of Competing Interest

The authors declare that they have no known competing financial interests or personal relationships that could have appeared to influence the work reported in this paper.

Data availability

Data will be made available on request.

Acknowledgements

Authors are grateful to Ruth Soto and two anonymous reviewers for their constructive comments, and to editor Christopher Fielding for his valuable advice. This paper was funded by projects PID2021-122612OB-I00 and Group E18 (Aragosaurus: Recursos Geológicos y Paleoambientes) subsidized by the Ministerio de Ciencia e Innovación, the European Regional Development Fund and the Government of Aragón. The Government of Aragón (Dirección General de Patrimonio Cultural) authorized the palaeontogical fieldwork campaigns (DGA Exp 080/20-21-2022). The research of Diego Torromé is funded by a DGA Grant (Aragón Department of Science, University, and Society of Knowledge). Manuel Pérez-Pueyo is funded by Ph.D grant from the Spanish Ministry of Education, Culture and Sport (Grant Number FPU 16/03064). The authors acknowledge the use of the SAI-Universidad de Zaragoza, and the advice of Elisabet Beamud of the paleomagnetism laboratory of the University of Barcelona.

References

Adrover, R., Feist, M., Hugueney, M., Mein, P., Moissenet, E., 1982. L'âge et la mise en relief de la formation detritique culminante de la Sierra Pelarda (Prov. Teruel, Espagne). C. R. Acad. Sci. Paris 295, 231–236.
Allen, J.R.L., 1983. Studies in fluviatile sedimentation: bars, bar complexes and sandstone sheets (low-sinuosity braided streams) in the brownstones (L. Devonian), Welsh Borders. Sediment. Geol. 33, 237–293.
Almunia, A., Arqued, V., Meléndez, A., 1985. Características sedimentarias durante el ciclo Senosiense en el Maestrazgo. Trabajos de geología (Universidad de Oviedo) 15, 159–169.
Alonso, A., Meléndez, N., Mas, J.R., 1991. Sedimentación lacustre durante el Cretácico en la Cordillera Ibérica, España. Acta Geol Hispánica 26, 35–54.
Alonso, A., Floquet, M., Mas, R., Meléndez, A., 1993. Late cretaceous carbonate platforms, origin and evolution, Iberian Range, Spain. In: JAT, Simó, Scott, R.W., Masse, J.P. (Eds.), Cretaceous Carbonate Platforms, pp. 297–313. American Association of Petroleum Geologists Memoir 56.
Alonso-Zarza, A.M., Calvo, J.P., 2000. Palustrine sedimentation in an episodically subsiding basin: the Miocene of the northern Teruel Graben (Spain). Palaeogeogr. Palaeoclimatol. Palaeoecol. 160, 1–21.
Alvaro, M., Capote, R., Vegas, R., 1979. Un Modelo de evolución geotectónica Para la Cadena Celtibérica. Act. Geol. Hispánica 14, 172–177.
Antolín-Tomás, B., Liesa, C.L., Casas, A., Gil-Peña, I., 2007. Geometry of fracturing linked to extension and basin formation in the Maestrazgo basin (Eastern Iberian Chain, Spain). Rev. Soc. Geol. España 20, 351–365.
Antunes, M.T., Pais, J., 1978. Notas sobre os depósitos de Taveiro, estratigrafia, paleontologia, idade, paleoecologia. Ciências da Terra 4, 109–128.
Antunes, M.T., Mateus, O., 2003. Dinosaurs of Portugal. Comptes Rendus Palevol. 2 (1), 77–95.
Aragües, L.M., Beltrán, F.J., Lanaja, J.M., Marín, J, 1981. Muniesa (467). Mapa Geológico de España E. 1:50.000. IGME Editor (Madrid) 1–25.
Armenteros, I.Corrochano, Alonso-Gavilán, G., Carballeira, J., Rodriguez, J.M., 2002. Duero basin (northern Spain). In: Gibbons, W., Moreno, M.T. (Eds.), The Geology of Spain, Chap. 13. The Geological Society, London, pp. 309–315.
Astibia, H., Corral, J.C., Murelaga, X., Orue-Etxebarria, X., Pereda-Suberbiola, X., coords, 1999. Geology and palaeontology of the Upper cretaceous vertebrate-bearing beds of the Laño quarry (Basque-Cantabrian Region, Iberian Peninsula). Estudios Museo de Ciencias Naturales de Alava 14 (Número Especial 1), 1–380.
Aurell, M., Robles, S., Bádenas, B., Quesada, S., Rosales, I., Meléndez, G., García-Ramos, J.C., 2003. Transgressive/regressive cycles and Jurassic palaeogeography of NE Iberia. Sed. Geology 162, 239–327.
Aurell, M., Soria, A.R., Bádenas, B., Liesa, C.L., Canudo, J.I., Gasca, J.M., Moreno-Azanza, M., Medrano-Aguado, E., Mélendez, A., 2018. Barremian synrift sedimentation in the Oliete subbasin (Iberian Basin, Spain): palaeogeographical evolution and distribution of vertebrate remains. J. Iberian Geology 44, 285–308.
Aurell, M., Fregenal-Martínez, M., Bádenas, B., Muñoz-García, M.B., Élez, J., Meléndez, N., De Santisteban, C., 2019. Middle Jurassic-early cretaceous tectono-sedimentary evolution of the southwestern Iberian Basin (central Spain): Major palaeogeographical changes in the geotectonic framework of the Western Tethys. Earth Sci. Rev. 199, 102–983.
Baceta, J.I., Pujalte, V., Orue-Etxebarria, X., 1999. The vertebrate fossil-bering sites of the Laño quarry (Basque-Cantabrian Region): Stratigraphical and palaeogeographical context. In: Estudios del Museo de Ciencias Naturales de Alava 14 (Número Especial 1), pp. 13–28.
Baceta, J.I., Pujalte, V., Bernaola, G., 2005. Paleocene coralgal reefs of the western Pyrenean basin, northern Spain: New evidence supporting an earliest Paleogene recovery of reefal ecosystems. Palaeogeogr. Palaeoclimatol. Palaeoecol. 224, 117–143.
Bardet, N., Corral, J.C., Pereda-Suberbiola, X., 1997. Les mosasaures (Squamata) du Crétacé supérieur du Bassin Basco-Cantabrique. Geobios 20, 19–26.
Barrier, E., Vrielynck, B., Brouillet, J.-F., Brunet, M.-F., 2018. Atlas of Paleotectonic Reconstruction of the Central Tethyan Realm. Tectono-Sedimentary-Palin- Spastic Maps from Late Permian to Pliocene. CCGM/CGMW, Paris.
Berreteaga, A., 2008. Estudio estratigráfico, sedimentológico y paleontológico de los yacimientos con fósiles de vertebrados del Cretácico final de la Región Vasco-Cantábrica. In: Univ. del País Vasco, p. 410 p.. PhD Thesis.
Berreteaga, A., Pereda, Suberbiola X., Floquet, M., Olivares, M., Etxebarria, N., Iriarte, E., Badiola, A., Elorza, J.J., Astibia, H., 2008. Datos sedimentológicos y tafonómicos de enclaves finicretácicos con fósiles de vertebrados de la Formación Sobrepeña (Burgos, Región Vasco-Cantábrica). Geotemas. 10, 1277–1280.
Berreteaga, A., Poyato, F.J., Pereda-Suberbiola, X., 2011. A new Actinopterygian fauna from the latest cretaceous of Quintanilla la Ojada (Burgos, Spain). Geodiversitas 33 (2), 285–301.
Brusatte, S.L., Butler, R.J., Barrett, P.M., Carrano, M.T., Evans, D.C., Lloyd, G.T., Mannion, P.D., Norell, M.A., Peppe, D.J., Upchurch, P., Williamson, T.E., 2015. The extinction of the dinosaurs. Biol. Rev. 90, 628–642.
Buscalioni, A.D., Martínez-Salanova, J., 1990. Los vertebrados fósiles del yacimiento de Armuña (Prov. Segovia, España). In: Comunicaciones Reunión de Tafonomía Y Fosilización, pp. 51–57. Madrid.
Butler, R.F., 1992. Paleomagnetism: Magnetic Domains to Geologic Terranes. Blackwell Scientific Publications.
Canudo, J.I., 2018. The collection of type fossils of the Natural Science Museum of the University of Zaragoza (Spain). Geoheritage 10, 385–392.
Canudo, J.I., Infante, P., Murelaga, X., 2005. Primer Registro de vertebrados continetales (Dinosauria y Quelonii) en el Maastrichtiense de Teruel (Cirugeda, Aliaga). Fundamental 6, 57–62.
Canudo, J.I., Oms, O., Vila, B., Galobart, À., Fondevilla, V., Puértolas-Pascual, E., Sellés, A.G., Cruzado-Caballero, P., Dinarès-Turell, J., Vicens, E., 2016. The upper Maastrichtian dinosaur fossil record from the southern Pyrenees and its contribution to the topic of the Cretaceous-Palaeogene mass extinction event. Cretac. Res. 57, 540–551.
Capote, R., Muñoz, J.A., Simón, J.L., Liesa, C.L., Arlegui, L.E., 2002. Alpine Tectonics I: the Alpine system North of the Betic Cordillera. In: Gibbons, W., Moreno, T. (Eds.), The Geology of Spain. The Geological Society, London, pp. 367–400.
Casas, A.M., Cortés, A.L., Liesa, C.L., Meléndez, A., Soria, A.R., 1997. Estructura del borde norte de la Cordillera Ibérica entre la Sierra de Arcos y el anticlinal de Montalbán. Cuadernos de Geología Ibérica 23, 243–268.
Casas, A.M., Pérez, A., Tena, S., Barrier, L., Gapais, D., Nalpas, T., 2000. Syn-tectonic sedimentation and thrust-and-fold kinematics at the intra-mountain Montalbán Basin (northern Iberian Chain, Spain). Geodin. Acta 13, 1–17.
Chadima, M., Hrouda, F., 2006. Remasoft 3.0 a user-friendly paleomagnetic data browser and analyzer. Travaux Géophysiques 27, 20–21.
Collinson, J., Mountney, N., 2019. Sedimentary Structures. In: Fourth edition. Dunedin Academic Press, p. 352p.
Company, J., 2004. Vertebrados continentales del Cretácico Superior (Campaniense-Maatrichtiense) de Valencia. Universitat de Valencia (Spain), 410 pp. Ph.D. thesis.
Company, J., 2017. Unusually thick dinosaur eggshell fragments from the Spanish late cretaceous. Hist. Biol. 31, 203–210.
Company, J., Szentesi, Z., 2012. Amphibians from the late cretaceous Sierra Perenchiza Formation of the Chera Basin, Valencia Province, Spain. Cretac. Res. 37, 240–245.
Company, J., Pereda-Suberbiola, X., Ruiz-Omeñaca, J.I., 2009. Nuevos restos fósiles del dinosaurio Lirainosaurus (Sauropoda, Titanosauria) en el Cretácico Superior (Campaniano-Maastrichtiano) de la Península Ibérica. Ameghiniana 46, 391–405.
Corral, J.C., Pueyo, E.L., Berreteaga, A., Rodríguez-Pinto, A., Sanchez, E., Pereda-Suberbiola, X., 2016. Magnetostratigraphy and lithostratigraphy of the Laño vertebrate-site: Implications in the uppermost cretaceous chronostratigraphy of the Basque-Cantabrian Region. Cretac. Res. 57, 473–489.
Csiki-Sava, Z., Buffetaut, E., Ösi, A., Pereda-Suberbiola, X., Brusatte, S.L., 2015. Island life in the Cretaceous: faunal composition, biogeography, evolution, and extinction of land-living vertebrates on the Late Cretaceous European archipelago. ZooKeys 469, 1–161.
Dercourt, J., Zonenshain, L.P., Ricou, L.E., Kazmin, V.G., Le Pichon, X., Knipper, A.L., Grandjacquet, C., Sbortshikov, I.M., Geyssant, J., Lepvrier, C., Pechersky, D.H., Boulin, J., Sibuet, J.-C., Savostin, L.A., Sorokhtin, O., Westphal, M., Bazhenov, M.L., Lauer, J.P., Biju-Duval, B., 1986. Geological evolution of the Tethys belt from the Atlantic to the Pamirs since the Lias. Tectonophysics 123, 241–315.
Dielforder, A., Frasca, G., Brune, S., Ford, M., 2019. Formation of the Iberian-European convergent plate boundary fault and its effect on intraplate deformation in Central Europe. Geochem. Geophys. Geosyst. 20, 2395–2417.

Díez-Díaz, V., Pereda-Suberbiola, X., Sanz, J.L., 2011. Braincase anatomy of the sauropod dinosaur Lirainosaurus astibiae (Titanosauria) from the late cretaceous of the Iberian Peninsula. Acta Paleontologica Polonica 56, 521–533.
Díez-Díaz, V., Pereda-Suberbiola, X., Sanz, J.L., 2013. The axial skeleton of the titanosaur Lirainosaurus astibiae (Dinosauria: Sauropoda) from the latest cretaceous of Spain. Cretac. Res. 43, 145–160.
Díez-Díaz, V., Pereda-Suberbiola, X., Company, J., 2015. Updating titanosaurian diversity (Sauropoda) from the late cretaceous of Spain: the fossil sites of Laño and Chera. Spanish J. Paleontol. 30, 293–306.
Díez Díaz, V., Mocho, P., Páramo, A., Escaso, F., Marcos-Fernández, F., Sanz, J.L., Ortega, F., 2016. A new titanosaur (Dinosauria, Sauropoda) from the Upper cretaceous of Lo Hueco (Cuenca, Spain). Cretac. Res. 68, 49–60.
Feist, M., Colombo, F., 1983. La limite Crétacé-Tertiaire dans le Nord-Est de l'Espagne, du point de vue des charophytes. Géologie Méditerranéenne 10, 303–326.
Feist, M., Floquet, M., 2022. Charophytes from the Upper cretaceous Castilian marine ramp and continental basins (central northern Spain): Fossil assemblages and depositional environments. Cretac. Res. 140, 105325.
Fernández-Garcia, P., Mas, R., Rodas, M., Luque del Villar, F.J., Garzón, G., 1989. Los depósitos aluviales del Paleógeno basal en el sector suroriental de la Cuenca del Duero (provincia de Segovia). Evolución y minerales de la arcilla característicos. Estud. Geol. 45, 27–43.
Floquet, M., 1991. La plate-forme Nord-castillane au Crétacé supérieur (Espagne). Arrière-pays ibérique de la marge passive basco-cantabrique. Sédimentation et Vie. Mémoires Géologiques Univ. Dijon 14, 925 pp.
Floquet, M., Alonso, A., Meléndez, A., 1982. Cameros-Castilla. El Cretácico Superior. In: García, A. (Ed.), El Cretácico de España, Madrid: Editorial Complutense, pp. 387–456.
Floquet, M., Salomon, J., Vadot, J.P., 1994. Uppermost Cretaceous and Paleogene fluvio-lacustrine basins in the northern Iberian Ranges (Spain). In: Gierlowski-Kordesch, E., Kelts, K. (Eds.), Global Geological Record of Lake Basins. Cambridge University Press, pp. 223–227. American Association of Petroleum Geologists Memoir 56.
Fondevilla, V., Riera, V., Vila, B., Sellés, A.G., Dinarès-Turell, J., Vicens, E., Gaete, R., Oms, O., Galobart, A., 2019. Chronostratigraphic synthesis of the latest cretaceous dinosaur turnover in South-Western Europe. Earth Sci. Rev. 191, 168–189.
Fryberger, S.G., Schenk, C.J., 1988. Pin stripe lamination: a distinctive feature of modern and ancient eolian sediments. Sediment. Geol. 55 (1–2), 1–15.
Galbrun, B., Feist, M., Colombo, F., Rocchia, R., Tambareau, Y., 1993. Magnetostratigraphy and biostratigraphy of Cretaceous-Tertiary continental deposits, Ager Basin, Province of Lerida, Spain. Palaeogeogr. Palaeoclimatol. Palaeoecol. 102, 41–52. https://doi.org/10.1016/0031-0182(93)90004-3.
Garcés, M., López-Blanco, M., Valero, L., Beamud, E., Muñoz, J.A., Oliva-Urcia, B., Vinyola, A., Cabello, P., Cabrera, L., 2020. Paleogeographic and sedimentary evolution of the south Pyrenean foreland basin. Mar. Pet. Geol. 113, 104105.
García, A., Mas, R., Segura, M., Carenas, B., García-Hidalgo, J.F., Gil, J., Alonso, A., Aurell, M., Bádenas, B., Benito, B.I., Meléndez, A., Salas, R., 2004. Segunda fase de post-rifting: Cretacico Superior. In: Vera, J.A. (Ed.), Geología de España. Sociedad Geológica de España, Instituto Geológico y Minero de España, pp. 510–522.
García-Penas, A., Aurell, M., Zamora, S., 2022. Progressive opening of a shallow-marine bay (Oliete Subbasin, Spain) and the record of possible eustatic fall events near the Barremian-Aptian boundary. Palaeogeogr. Palaeoclimatol. Palaeoecol. 594, 110938.
Garrido-Megías, A., 1973. Estudio geológico y relación entre tectónica y sedimentación del Secundario y Terciario de la vertiente meridional pirenaica en su zona central (provincias de Huesca y Lérida). Universidad de Granada, 395 pp. PhD Thesis.
Gautier, P.W., 1980. Memoria explicativa de la Hoja núm. 543 (Villarluengo. In: Mapa geológico de España 1:50.000, segunda serie. Instituto Geológico de España (IGME), Madrid.
Gil, J., Carenas, B., Segura, M., García-Hidalgo, J.F., García, A., 2004. Revisión y correlación de las unidades litoestratigráficas del Cretácico Superior en la región central de España. Rev. Soc. Geol. Esp. 17, 249–266.
Gil, J., Segura, M., García-Hidalgo, J.F., López-Olmedo, F., 2010. El Cretácico del Sistema Central (España): Registro estratigráfico, contexto deposicional y esquema evolutivo. Boletín de la Real Sociedad Española de Historia Natural 104, 15–36.
Gómez-Gras, D., Roige, M., Fondevilla, V., Oms, O., Boya, S., Remacha, E., 2016. Provenance constraints on the Tremp Formation paleogeography (southern Pyrenees): Ebro Massif vs Pyrenees sources. Cretac. Res. 57, 414–427.
González, A., 1989. Análisis tectosedimentario del Terciario del borde SE de la Depresión del Ebro (sector bajoaragonés) y cubetas ibéricas marginales. Universidad de Zaragoza, 507 pp. PhD Thesis.
González, A., Guimer, À.J., 1993. Sedimentación sintectónica en una cuenca transportada sobre una lámina de cabalgamiento: la cubeta Terciaria de Aliaga. Rev. Soc. Geol. España 6, 151–165.
Gónzalez, A., Pérez, A., 2018. El Terciario del sector turolense de la Cuenca del Ebro: una crónica de la estructuración alpina de la Cordillera Ibérica. In: Alcala, L., Calvo, J.P., Simon, J.L. (Eds.), Geología de Teruel. Instituto de Estudios Turolenses, pp. 83–98.
Grambast, L., 1975. Charophytes du Crétacé supérieur de la région de Cuenca. In: Caja Provincial de Ahorros de Cuenca (ed.) I Simposium del Cretácico de la Cordillera Ibérica. Imprenta Magerit, Madrid, pp. 67–83.
Grambast, L., Gutiérrez, G., 1977. Espèces nouvelles de charophytes du Crétacé supérieur terminal de la Province de Cuenca (Espagne). Paléobiologie Continentale 8, 1–34.
Guimerà, J., 2018. Structure of an intraplate fold-and-thrust belt: the Iberian Chain.A synthesis. Geologica Acta 16, 427–438.
Guimerà, J., Mas, R., Alonso, A., 2004. Intraplate deformation in the NW Iberian Chain: Mesozoic extension and Tertiaty contractional inversion. J. Geol. Soc. 161, 291–303.
Gutiérrez, G., Robles, F., 1976. Biostratigraphie du Sénonien continental des environs de Villalba de la Sierra (province de Cuenca, Espagne). Paléobiologie Continentale 7, 11–17.
Haq, B.U., 2014. Cretaceous eustasy revisited. Glob. Planet. Chang. 113, 44–58.
Hardie, L.A., Smoot, J.P., Eugster, H.P., 1978. Saline Lakes and their deposits: a Sedimentological Approach. In: Matter, A., Tucker, M.E. (Eds.), Modern and Ancient Lake Sediments. International Association of Sedimentologists, pp. 7–41.
Herrero, C., Herrero, E., Martín-Chivelet, J., Pérez-Lorente, F., 2016. Contribution to knowledge of the last dinosaur footprints in Europa. Persistence of ornithopods in the upper Maastrichtian of SE Spain. Cretac. Res. 57, 490–507.
Huerta, P., Armenteros, I., Recio, C., Blanco, J.A., 2010. Palaeogroundwater evolution in playa–lake environments: sedimentary facies and stable isotope record (Palaeogene, Almazán Basin, Spain). Palaeogeogr. Palaeoclimatol. Palaeoecol. 286 (3–4), 135–148.
Huerta, P., Armenteros, I., Silva, P.G., 2011. Large-scale architecture in non-marine basins: the response to the interplay between accommodation space and sediment supply. Sedimentology 58 (7), 1716–1736.
Isasmendi, E., Torices, A., Canudo, J.I., Currie, P.J., Pereda-Suberbiola, X., 2022. Upper cretaceous european theropod palaeobiodiversity, palaeobiogeography and the intra-Maastrichtian faunal turnover: new contributions from the Iberian fossil site of Laño. Papers in Palaeontology 8, e1419.
Kirschvink, J.L., 1980. The least-squares line and plane and the analysis of palaeomagnetic data. Geophys. J. R. Astron. Soc. 62, 699–718.
Laita, E., Bauluz, B., Aurell, M., Bádenas, B., Canudo, J.I., Yuste, A., 2020. A change from warm/humid to cold/dry climate conditions recorded in lower Barremian clay-dominated continental successions from the SE Iberian Chain (NE Spain). Sediment. Geol. 403, 105673.
Lapparent, A.F., de Quintero, L., Trigueros, E., 1957. Descubrimientos de huesos de dinosaurios en el Cretáceo terminal de Cubilla (Provincia de Soria). Notas y Comunicaciones del lnst. Geol. y Minero de España 45, 3–5.
Le Loeuff, J., Buffetaut, E., Martin, M., 1994. The last stages of dinosaur faunal history in Europe: a succession of Maastrichtian dinosaur assemblages from the Corbières (southern France). Geol. Mag. 131, 625–630.
Liesa, C.L., Casas, A.M., Simón, J.L., 2018. La tectónica de inversión en una región intraplaca: La Cordillera Ibérica. Rev. Soc. Geol. España 31, 23–50.
Llompart, C., Casanovas, M.L., Santafé, J.V., 1984. Un nuevo yacimiento de icnitas de dinosaurios en las facies garumnienses de la Conca de Tremp (Lleida, España). Acta Geológica Hispánica 19, 143–147.
López-Martínez, N., Canudo, J.I., Ardèvol, L., Pereda-Suberbiola, X., Orue-Etxebarria, X., 2001. New dinosaurs sites correlated with the Upper Maastrichtian pelagic deposits in the Spanish Pyrenees: implications for the dinosaur extinction pattern in Europe. Cretac. Res. 22, 41–61.
Marmi, J., Martín-Closas, C., Fernández-Marrón, M.T., Fondevilla, V., Gomez, B., 2015. A riparian plant community from the upper Maastrichtian of the Pyrenees (Catalonia, NE Spain). Cretac. Res. 56, 510–529.
Martín-Chivelet, J., 1994. Litoestratigrafía del Cretácico Superior del Altiplano de Jumilla-Yecla (Zona Prebética). Cuadernos de Geología Ibérica 18, 117–173.
Martín-Chivelet, J., Giménez, R., 1992. Palaeosols in microtidal carbonate sequences: Sierra de Utiel Formation, Upper cretaceous, SE Spain. Sediment. Geol. 81, 125–145.
Martín-Chivelet, J., Berástegui, X., Rosales, I., Vilas, L., Vera, J.A., Caus, E., Gräfe, K.U., Mas, R., Puig, C., Segura, M., Robles, S., Floquet, M., Quesada, S., Ruiz-Ortiz, A., Fregenal-Martínez, M.A., Salas, R., Arias, C., García, A., Martín-Algarra, A., Meléndez, M.N., Chacón, B., Molina, J.M., Sanz, J.L., Castro, J.M., García-Hernández, M., Carenas, B., García-Hidalgo, J., Gil, J., Ortega, F., 2002. Cretaceous. In: Gibbons, W., Moreno, M.T. (Eds.), Geology of Spain. The Geological Society, London, pp. 255–292.
Martín-Chivelet, J., Floquet, M., García-Senz, J., Callapez, P.M., López-Mir, B., Muñoz, J. A., Dinis, P.M., 2019a. Late Cretaceous post-rift to convergence in Iberia. In: The Geology of Iberia: A Geodynamic Approach. Springer, Heidelberg, pp. 285–376.
Martín-Chivelet, J., López-Gómez, J., Aguado, R., Arias, C., Arribas, J., Arribas, M.E., Aurell, M., Bádenas, B., Benito, M.I., Bover-Arnal, T., Casas-Sainz, A., Castro, J.M., Coruña, F., de Gea, G.A., Fornós, J.J., Fregenal-Martínez, M., García-Senz, J., Garófano, D., Gelabert, B., Giménez, J., González-Acebrón, J., Guimerà, J., Liesa, C. L., Mas, R., Meléndez, N., Molina, J.M., Muñoz, J.A., Navarrete, R., Nebot, M., Nieto, L.M., Omodeo-Salé, S., Pedrera, A., Peropadre, C., Quijada, I.E., Quijano, M.L., Reolid, M., Robador, A., Rodríguez-López, J.P., Rodríguez-Perea, A., Rosales, I., Ruiz-Ortiz, P.A., Sàbat, F., Salas, R., Soria, A.R., Suarez-Gonzalez, P., Vilas, L., 2019b. The late Jurassic–early cretaceous rifting. In: Quesada, C., Oliveira, J.T. (Eds.), The Geology of Iberia: A Geodynamic Approach, The Alpine Cycle, Volume 3. Springer, Heidelberg, pp. 170–250.
Miall, A.D., 1977. A review of the braided river depositional environment. Earth Sci. Rev. 13 (1–61).
Moreno-Azanza, M., Bauluz, B., Canudo, J.I., Gasca, J.M., Torcida, F., 2016. Combined use of electron and light microscopy techniques reveals false secondary shell units in megaloolithidae eggshells. PLoS ONE 11 (5), e0153026.
Muñoz, A., Arenas, C., González, A., Luzón, A., Pardo, G., Pérez, A., Villena, J., 2002. Ebro basin (northeastern Spain). In: Gibbons, W., Moreno, T. (Eds.), The Geology of Spain. The Geological Society, London, pp. 301–309.
Neres, M., Font, E., Miranda, J.M., Camps, P., Terrinha, P., Mirão, J., 2012. Reconciling cretaceous paleomagnetic and marine magnetic data for Iberia: new Iberian paleomagnetic poles. J. Geophys. Res. 117, B06102.
Nichols, G.J., 2005. Sedimentary evolution of the Lower Clair Group, Devonian, west of Shetland: climate and sediment supply controls on fluvial, aeolian and lacustrine deposition. In: Doré, A.G., Vining, B.A. (Eds.), Petroleum Geology: North West Europe and Global Perspectives - Proceedings of the 6th Petroleum Geology Conference. Geological Society, London, pp. 957–967.
Nichols, G.J., Fisher, J.A., 2007. Processes, facies and architecture of fluvial distributary system deposits. Sediment. Geol. 195 (1–2), 75–90.

Ogg, J.G., 2012. Geomagnetic polarity time scale. In: The Geologic Time Scale. Elsevier, pp. 85–113.
Ortega, F., Pérez-García, A., 2009. Cf. Lirainosaurus sp. (Dinosauria: Titanosauria) en el Cretácico Superior de Sacedón (Guadalajara). Geogaceta 46, 87–90.
Ortega, F., Bardet, N., Barroso-Barcenilla, F., Callapez, P.M., Cambra-Moo, O., Daviero-Gómez, V., et al., 2015. The biota of the Upper cretaceous site of "Lo Hueco" (Cuenca, Spain). J. Iber. Geol. 41, 83–99.
Osete, M.L., Palencia Ortas, A., Luisa, M., Sete, O., Alencia, A.P., 2006. Polos Paleomagnéticos de Iberia de los últimos 300 millones de años. Física la Tierra 157–181.
Pardo, G., Villena, J., González, A., 1989. Contribución a los conceptos y a la aplicación del análisis tectosedimentario, Rupturas y unidades tectosedimentarias Como fundamento de correlaciones estratigráficas. Rev. Soc. Geol. España 2, 199–221.
Pardo, G., Arenas, C., González, A., Luzón, A., Muñoz, A., Pérez, A., Pérez-Rivarés, F.J., Vázquez-Urbez, M., Villena, J., 2004. La Cuenca del Ebro. In: Vera, J.A. (Ed.), Geología de España. SGE-IGME, Madrid, pp. 533–543.
Pereda-Suberbiola, X., Ruiz-Omeñaca, J.I., 2001. Un dinosaurio saurópodo (Titanosauria) en el Cretácico superior de Cubilla, Soria (España). Geogaceta 30, 175–178.
Pereda-Suberbiola, X., Astibia, H., Murelaga, X., Elorza, J.J., Gómez-Alday, J.J., 2000. Taphonomy of the late cretaceous dinosaur-bearing beds of the Laño Quarry (Iberian Peninsula). Palaeogeogr. Palaeoclimatol. Palaeoecol. 157, 247–275.
Pereda-Suberbiola, X., Ruiz-Omeñaca, J.I., Company, J., 2003. Los dinosaurios hadrosaurios del registro ibérico. Descripción de nuevo material del Cretácico superior de Laño (Condado de Treviño). In: Pérez-Lorente, F. (Ed.), Dinosaurios Y Otros Reptiles Mesozoicos en España, Vol. 26. Logroño. Ciencias de la Tierra, Instituto de Estudios Riojanos (IER), pp. 375–388.
Pereda-Suberbiola, X., Corral, J.C., Astibia, H., Badiola, A., Bardet, N., Berreteaga, A., Buffetaut, E., Buscalioni, A.D., Cappetta, H., Cavin, L., Díez, Díaz V., Gheerbrant, E., Murelaga, X., Ortega, F., Pérez-García, A., Poyato-Ariza, F., Rage, J.-C., Sanz, J.L., Torices, A., 2015. Late cretaceous continental and marine vertebrate assemblages from the Laño Quarry (Basque-Cantabrian Region, Iberian Peninsula): an update. J. Iber. Geol. 41, 101–124.
Pérez, A., Pardo, G., Villena, J., González, A., 1983. Estratigrafía y Sedimentología del Paleógeno de la cubeta de Montalbán (prov. de Teruel, España). Bol. R. Soc. Española Hist. Nat. (Geol.) 81, 197–223.
Pérez-García, A., Ortega, F., Bolet, A., Escaso, F., Houssaye, A., Martínez-Salanova, J., de Miguel Chaves, C., Mocho, P., Narváez, I., Segura, M., Torices, A., Vidal, D., Sanz, J. L., 2016. A review of the upper Campanian vertebrate site of Armuña (Segovia Province, Spain). Cretac. Res. 57, 591–623.
Pérez-Pueyo, M., Cruzado-Caballero, P., Moreno-Azanza, M., Vila, B., Castanera, D., Gasca, J.M., Puértolas-Pascual, E., Bádenas, B., Canudo, J.I., 2021. The tetrapod fossil record from the uppermost Maastrichtian of the Ibero-Armorican Island: an integrative review based on the outcrops of the western Tremp Syncline (Aragón, Huesca Province, NE Spain). Geosciences 11, 162.
Pérez-Rivares, J., Arenas, C., Pardo, G., Garcés, M., 2018. Temporal aspects of genetic stratigraphic units in continental sedimentary basins: examples from the Ebro basin, Spain. Earth-Sci. Rev. 178, 136–153.
Peyrot, D., Barroso-Barcenilla, F., Cambra-Moo, 2013. Paleoecology of the late Campanian/early Maastrichtian Fossil-Lagerstätte of "Lo Hueco" (Cuenca, Spain): palynological insights. Palaeogeogr.Palaeoclimatol. Palaeoecol. 387, 27–39.
Peyrot, D., Barrón, E., Pereda-Suberbiola, X., Company, J., 2020. Vegetational composition of the Upper cretaceous vertebrate site of Chera (Valencia, Spain) and its significance in mosaic vegetation from southwestern Europe. Cretac. Res. 106, 104254.
Pueyo, E.L., Pereda Suberbiola, X., Company, J., Sanchez, E., Berreteaga, A., Corral, J.C., 2014. Magnetostratigraphy of the latest Cretaceous vertebrate-bearing sites from the Basque-Cantabrian Region and eastern Iberian Range: Preliminary data. In: Marmi, J., Oms, O., Vila, B., Galobart, A., Estrada, R., Dinares-Turell, J. (Eds.), Reconstructing the Terrestrial End-Cretaceous Palaeoenvironments in Europe, Tremp, September 16-20th 2014, Field Trip Guide and Abstracts Book. Paleontologia i Evolucio ME 7, p. 76.
Puigdefàbregas, C., Muñoz, J.A., Marzo, M., 1986. Thrust belt development in the eastern Pyrenees and related depositional sequences in the southern foreland basin. In: Allen, P.A., Homewood, P. (Eds.), Foreland Basins, Spec. Publs. Int. Ass. Sediment. 8. Blackwell Publishing Ltd, Oxford, UK, pp. 229–246.
Ramos, A., Sopeña, A., 1983. Gravel bars in low-sinuosity streams (Permian and Triassic, Central Spain). Special Publication of the International Association of Sedimentologists 6, 301–312.
Riera, V., Oms, O., Gaete, R., Galobart, À., 2009. The end-cretaceous dinosaur succession in Europe: the Tremp Basin record (Spain). Palaeogeogr. Palaeoclimatol. Palaeoecol. 283, 160–171.
Ríos-Aragües, L.M., Lanaja, J.M., Marín, J., 1981. Memoria explicativa de la Hoja núm. 467 (Muniesa). In: Mapa geológico de España 1:50.000, segunda serie. Instituto Geológico de España (IGME), Madrid.
Salgado, L., Calvo, J.O., 1993. Report of a sauropod with amphiplatyan mid-caudal vertebrae from the late cretaceous of Nequen Province (Argentina). Ameghiniana 30 (2), 215–218.
Salgado, L., Coria, R.A., Calvo, J.O., 1997. Evolution of titanosaurid sauropods. I: Phylogenetic analysis based on the postcranial evidence. Ameghiniana 34, 1, 3–32.
Sanguino, F., Gascó-Lluna, F., Pérez-García, A., Ortega, F., 2021. Ootaxonomy of the upper cretaceous dinosaur eggs from poyos (Sacedón, Guadalajara, Spain). Lucas Mallada 23, 223–224.
Santanach, P., 1989. Reflexiones sobre los mecanismos de incidencia de la Tectónica en la división estratigráfica de rellenos decuenca. Implicaciones en la correlación estratigráfica. Rev. Soc. Geol. Esp. 2, 223–234.
Santolaria, P., Luzón, A., Casas, A.M., Soto, R., 2015. Coupling far and near tectonic signals in syn-orogenic sediments: the Olvena growth strata (Sierras Marginales, southern Pyrenees). Geol. Acta 13 (4), 297–308.
Sanz, J.L., Powell, J.E., Le Loeuff, J., Martínez, R., Pereda Suberbiola, X., 1999. Sauropod remains from the Upper cretaceous of Laño (Northcentral Spain). Titanosaur phylogenetic relationships. Estudios del Museo de Ciencias Naturales de Álava 14, 235–255.
Sellés, A.G., Vila, B., 2015. Re-evaluation of the age of some dinosaur localities from the southern Pyrenees by means of megaloolithid oospecies. J. Iber. Geol. 41 (1), 125–139.
Simón, J.L., Liesa, C.L., 2011. Incremental slip history of a thrust: diverse transport directions and internal folding of the Utrillas thrust sheet (NE Iberian Chain, Spain). In: Poblet, J., Lisle, R.J. (Eds.), Kinematic evolution and Strucutral Styles of Fold-and-Thrust Belts, Geol. Soc. of London, Spec. Publ. 349, pp. 77–97.
Tauxe, L., Shaar, R., Jonestrask, L., Swanson-Hysell, N.L., Minnett, R., Koppers, A.A.P., Constable, C.G., Jarboe, N., Gaastra, K., Fairchild, L., 2016. PmagPy: Software package for paleomagnetic data analysis and a bridge to the Magnetics Information Consortium (MagIC) Database. GeochGeophys. Geosystems 17, 2450–2463.
Tauxe, L., 2010. Essentials of Paleomagnetism. University of California Press Ltd, Berkeley.
Torromé, D., Aurell, M., Bádenas, B., 2022. A mud-dominated coastal plain to lagoon with emerged carbonate mudbanks: the imprint of low-amplitude sea level cycles (mid-Upper cretaceous, South Iberian Ramp). Sediment. Geol. 476, 106178.
Vacherat, A., Mouthereau, F., Pik, R., Huyghe, D., Paquette, J.L., Christophoul, F., Loget, N., Bouchaib, T., 2017. Rift-to-collision sediment routing in the Pyrenees: a synthesis from sedimentological, geochronological and kinematic constraints. Earth-Sci. Rev. 172, 43–74.
Vandamme, D., 1994. A new method to determine paleosecular variation. Phys. Earth Planet. Inter. 85, 131–142.
Vegas, R., de Vicente, G., Casas-Sainz, A., Cloetingh, A.P.L., 2019. Alpine orogeny: intraplate defromation. In: The Geology of Iberia: A Geodynamic Approach. Springer, Cham, pp. 507–544.
Vianey-Liaud, M., López-Martínez, N., 1997. Late cretaceous dinosaur eggshells from the Tremp Basin, Southern Pyrenees, Lleida, Spain. J. Paleontol. 71, 1157–1171.
Vicente, A., Martín-Closas, C., Arz, J.A., Oms, O., 2015. Maastrichtian–basal Paleocene charophyte biozonation and its calibration to the Global Polarity Time Scale in the Southern Pyrenees (Catalonia, Spain). Cretac. Res. 52, 268–285.
Vicente, A., Villalba-Breva, S., Ferràndez-Cañadell, C., Martín-Closas, C., 2016. Charophyte biostratigraphy in the Fontllonga type section. Geol. Acta 14, 349–362.
Vicente, A., Csiki-Sava, Z., Martín-Closas, C., 2019. European charophyte evolution across the Cretaceous-Paleogene boundary. Palaeogeogr. Palaeoclimatol.Palaeoecol. 533, 109244.
Vila, B., Oms, O., Marmi, J., Galobart, À., 2008. Tracking Fumanya footprints (Maastrichtian, Pyrenees): historical and ichnological overview. Oryctos 8, 130–150.
Vila, B., Oms, O., Fondevilla, V., Gaete, R., Galobart, Á., Riera, V., Canudo, J.I., 2013. The latest succession of dinosaur tracksites in Europe: hadrosaur ichnology, track production and palaeoenvironments. PLoS ONE 8 (9), e72579.
Vila, B., Sellés, A.G., Brusatte, S.L., 2016. Diversity and faunal changes in the latest cretaceous dinosaur communities of South-Western Europe. Cretac. Res. 57, 552–564.
Vila, B., Selles, A., Moreno-Azanza, M., Razzolini, N.L., Gil-Delgado, A., Canudo, J.I., Galobart, A., 2022. A titanosaurian sauropod with Gondwanan affinities in the latest cretaceous of Europe. Nat. Ecol. Evol. 6, 288-29.
Vilas, L., Mas, R., García, A., Arias, C., Alonso, A., Meléndez, N., Rincón, R., 1982. La Cordillera Ibérica Suroccidental. In: Cretácico, El (Ed.), García a. Universidad Complutense de Madrid, de España, pp. 457–514.
Villalba-Breva, S., Martín-Closas, C., 2013. Upper cretaceous paleogeography of the Central Southern Pyrenean Basins (Catalonia, Spain) from microfacies analyses and charophyte biostratigraphy. Facies 5, 319–345.
Villalba-Breva, Martín-Closas, Marmi, J., Gomez, B., Fernández-Marrón, M.T., 2012. Peat-forming plants in the Maastrichtian coals of the Eastern Pyrenees. Geol. Acta 10, 189–207.
Villena, J., Pardo, G., Pérez, A., Muñoz, A., Gonzalez, A., 1996. The Tertiary of the Iberian margin of the Ebro basin: sequence stratigraphy. In: Friend, P.F., Dabrio, C.J. (Eds.), Tertiary Basins of Spain: The Stratigraphic Record of Crustal Kinematics. Cambridge University Press, pp. 77–82.
Visser, R.L.M., Meijer, P.Th., 2012. Mesozoic rotation of Iberia: subduction in the Pyrenees? Earth Sci. Rev. 110, 93–110.